

LLMs generate structurally realistic social networks but overestimate political homophily

Serina Chang^{1,*}, Alicja Chaszczewicz^{1,*}, Emma Wang¹,
Maya Josifovska^{1,2}, Emma Pierson³, Jure Leskovec¹

¹Department of Computer Science, Stanford University

²Department of Computer Science, University of California, Los Angeles

³Department of Computer Science, Cornell University

*These authors contributed equally.

Abstract

Generating social networks is essential for many applications, such as epidemic modeling and social simulations. Prior approaches either involve deep learning models, which require many observed networks for training, or stylized models, which are limited in their realism and flexibility. In contrast, LLMs offer the potential for zero-shot and flexible network generation. However, two key questions are: (1) are LLM’s generated networks realistic, and (2) what are risks of bias, given the importance of demographics in forming social ties? To answer these questions, we develop three prompting methods for network generation and compare the generated networks to real social networks. We find that more realistic networks are generated with “local” methods, where the LLM constructs relations for one persona at a time, compared to “global” methods that construct the entire network at once. We also find that the generated networks match real networks on many characteristics, including density, clustering, community structure, and degree. However, we find that LLMs emphasize political homophily over all other types of homophily and *overestimate* political homophily relative to real-world measures.

1 Introduction

The ability to generate realistic social networks is crucial for many applications, when the true social network cannot be observed (e.g., for privacy reasons) or a realistic network is desired between hypothetical individuals. For example, in epidemic modeling, synthetic social networks are frequently used so that researchers can model the spread of disease based on who has come into contact with whom (Barrett et al., 2009; Block et al., 2020). Synthetic networks are also useful for simulating and analyzing social media platforms (Pérez-Rosés and Sebé, 2015; Sagduyu et al., 2018) and social phenomena, such as polarization and opinion dynamics (Dandekar et al., 2013; Das et al., 2014).

Deep learning approaches to network generation typically require training on many domain-specific networks (You et al., 2018), making it difficult to generalize to new settings where networks are not yet observed. Classical models for network generation require far less training, but these stylized models make rigid and unrealistic assumptions about how networks form. For example, Erdős–Rényi models assume that each edge forms with a uniform probability p (Erdős and Rényi, 1959). More realistic models, like small-world models (Watts and Strogatz, 1998) or stochastic block models (Holland et al., 1983), are still limited by a predefined, small set of numerical hyperparameters, missing the full complexity of real social interactions.

In contrast, generating social networks with large language models (LLMs) has the potential to address these limitations. LLMs possess zero-shot capabilities, enabling network generation without training. LLMs can also generate networks in a flexible manner, based on natural language descriptions of each person in the network. A key question, however, is whether LLMs can generate *realistic* social networks. On one hand, LLMs have demonstrated capabilities to realistically simulate human responses and interactions (Aher et al., 2023; Park et al., 2023; Argyle et al., 2023), suggesting that they may be able to generate realistic social networks as well. On the other hand, LLMs sometimes struggle with reasoning over graphs (Wang et al., 2023; Fatemi et al., 2024) and it is unclear if their language abilities generalize to structured objects like networks, so that they can reproduce structural characteristics of social networks such as low density and long-tailed degree distributions.

Furthermore, a central concern with using LLMs in social settings is bias. Prior works have shown that LLMs produce stereotyped descriptions of individuals based on their demographics (Cheng et al., 2023a,b) and skew towards the liberal opinions (Santurkar et al., 2023). These demographics,

such as gender and political affiliation, play essential roles in the formation of real-world social networks, resulting in well-documented demographic homophily (McPherson et al., 2001; Kossinets and Watts, 2009). Thus, we cannot evaluate whether LLMs’ social network generation is realistic without incorporating demographics into our experiments; at the same time, we need to analyze how LLMs reason about these demographic features and investigate potential signs of bias.

The goal of this work is to study these two issues—realism and bias—in the context of social network generation with LLMs. Our research questions are as follows:

RQ1: Can LLM-generated networks match real-world social networks on structural characteristics? How do different prompting methods result in different network structures?

RQ2: Can LLMs capture demographic homophily? How do levels of homophily vary across demographic variables, and are there signs of bias?

RQ3: How does incorporating interests, beyond demographics, affect LLM-generated networks?

To answer these questions, we propose three prompting methods for social network generation (Figure 1). First, we find that “local” methods, where the LLM takes on the perspective of one person at a time, yield more realistic networks than “global” methods, where the LLM constructs the entire network at once, even though the LLM receives less information in the local setting. The LLM is able to generate networks that match real networks on many structural characteristics, including density, clustering, connectivity, and degree distribution. The LLM also exhibits clear demographic homophily, across gender, age, race/ethnicity, religion, and political affiliation. However, the LLM consistently emphasizes homophily in political affiliation above all other demographic variables, and overestimates levels of political homophily compared to reported levels in real online *and* offline social networks. Finally, we find that incorporating LLM-generated interests does not reduce political homophily, since the interests themselves encode political stereotypes. Overall, our work demonstrates the promise of using LLMs for social network generation while calling attention to challenges around integrating demographics.¹

¹Our code is available at <https://github.com/snap-stanford/llm-social-network>, along with our generated personas and generated social networks.

2 Related work

Social simulation with LLMs. Prior work has demonstrated LLMs’ abilities to realistically simulate human responses and interactions (Aher et al., 2023; Park et al., 2023; Argyle et al., 2023). However, while simulating interactions over networks, existing work focuses less on using LLMs to generate the networks themselves, either making simplistic assumptions about the network structure such as sampling agents randomly to interact (Park et al., 2022; Chuang et al., 2023) or requiring human involvement in building the network (Gao et al., 2023; Zhou et al., 2024). To improve the realism and usability of these simulations, it is essential to also explore LLMs’ abilities to *generate* the network structure, a prerequisite to simulating interactions over networks.

A few contemporaneous works have explored LLMs for social network generation, with different focuses from ours. Marzo et al. (2023) focus on degree distribution, showing that scale-free networks emerge from interactions between LLMs. He et al. (2023) focus on content homophily, analyzing a simulated society powered by LLM chatbots. The most similar work to ours is Papachristou and Yuan (2024), who analyze whether LLMs demonstrate network formation principles, such as preferential attachment and homophily. While their work establishes the existence of *general* network principles, our work compares generated networks to real social networks directly, computing many network metrics, and shows that all metrics can be matched at once, while their experiments primarily explore one principle at a time, with a different prompt for each principle. Also, to test homophily, they consider hobby, favorite color, and location, while we explore key demographic features.

LLM social biases. Using LLMs in social contexts raises concerns of biases and stereotyping (Cheng et al., 2023a,b; Wang et al., 2024). When responding to public opinion or political questions, LLMs’ answers skew liberal (Santurkar et al., 2023; Hartmann et al., 2023). When assigned a persona, LLMs show worse reasoning capabilities when assigned certain demographics (Gupta et al., 2024) and produce more toxic content under certain personas (Deshpande et al., 2023). However, bias in the context of social network generation remains unexplored. In this work, we investigate such biases by studying the effects of demographic variables on LLM-generated social networks.

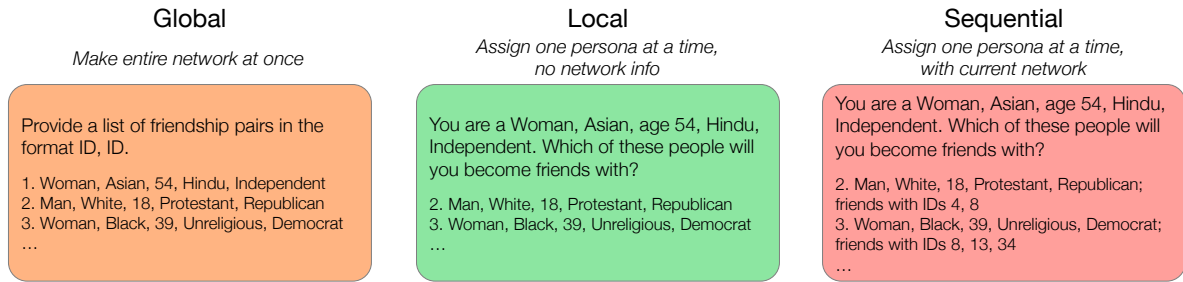


Figure 1: Our three prompting methods to generate social networks with LLMs. See full prompts in Figures 17-19.

Graph generation. Classical models for network generation do not require much training, but their simplicity often results in unrealistic network structures. For example, Erdős–Rényi models assume that each edge forms with uniform probability (Erdős and Rényi, 1959), Watts–Strogatz models (Watts and Strogatz, 1998) generate small-world networks but struggle to produce realistic degree distributions, and Barabási–Albert models (Barabási and Albert, 1999) capture power-law degree distributions but miss community structure and clustering. In contrast, machine learning approaches aim to learn graph generation directly from observed data, resulting in more realistic generated networks (You et al., 2018; Simonovsky and Komodakis, 2018; Guo and Zhao, 2023). However, these models require a set of training networks, and typically have fixed feature sets, so they cannot be applied in situations without access to real-world network data, and cannot be easily extended to incorporate new features, while LLMs can be.

LLMs & graphs. The use of LLMs has been explored for various graph tasks (Li et al., 2024; Jin et al., 2024), such as graph reasoning (Wang et al., 2023; Fatemi et al., 2024), node classification (Zhao et al., 2023; Chen et al., 2024; Ye et al., 2024), or tasks on knowledge graphs (Pan et al., 2024). These works have shown that LLMs possess preliminary graph reasoning capabilities, but struggle on larger graphs or harder tasks, such as finding a Hamilton path (Wang et al., 2023). Yao et al. (2024) is one of the first to explore LLMs for graph generation, but they explore it in the context of molecule generation, not social networks.

3 Generating social networks

Our process for generating social networks involves two steps: first, constructing a set of personas, and second, having the LLM generate social networks over those personas. In this section, we summarize

the two steps, with details in Appendix C.

3.1 Persona construction

For each persona, we include their gender, age, race/ethnicity, religion, and political affiliation, which are salient dimensions of homophily in real social networks (McPherson et al., 2001; Halberstam and Knight, 2016). We sample these characteristics based on the distribution of the US population. Using US Census data (US Census Bureau, 2023), we acquire the joint distribution for gender, age, and race/ethnicity. Then, we sample the persona’s religion, conditioned on their race/ethnicity (Statista, 2016; PRRI Staff, 2021), and political affiliation, conditioned on their gender and race/ethnicity (Pew Research Center, 2024; Sanchez and Foxworth, 2022). In Section 5.3, we also experiment with including interests for each persona, instead of only demographic variables.

3.2 Network generation

We design three prompting methods for generating social networks, which we summarize in Figure 1.

Global. In our first method, which we call “Global”, we provide the LLM with the entire list of personas, and prompt it to construct the network between them, in the form of edge pairs.

Local. In our second method, which we call “Local”, we have the LLM take on the identity of one persona at a time, e.g., by saying, “You are a Woman, Asian, age 54, Hindu, Independent.” We provide the LLM with the list of all other personas (in the same format) and prompt it to pick friends for the persona it is currently assigned. To construct the entire network, we iterate through all personas in a random order, and we keep an edge between personas A and B if the LLM selects B when acting as A or vice versa (so we do not require both to select each other). This method is inspired by techniques in machine learning that similarly model

the graph generation process by iterating through nodes and selecting edges for each node at a time (You et al., 2018).

Sequential. In our third method, we also assign the LLM one persona at a time, but in addition to providing the list of all other personas, we also provide information about the constructed graph so far. We experiment with providing each persona’s full list of current friends vs only their degree (i.e., total number of friends). These variations are similar to the preferential attachment experiments in Papachristou and Yuan (2024), where they also experimented with providing neighborhood information vs. only degree, although their experiments only considered the network and no demographic features. In contrast, our experiments—and in particular, the comparison of the Local to Sequential methods—reveal how providing demographic and network information compare to only providing demographic information.

4 Comparison to real networks

To evaluate the realism of our generated networks, we gather a set of real social networks from the CASOS² and KONECT³ repositories. We kept networks that described social relations between individuals, which filtered out other types of networks, such as work-related interactions or visiting ties between families. We included eight real networks, which capture social ties within diverse communities, including physicians, students, and prisoners (see Appendix C.3 for details).

We extract graph-level and node-level metrics from the real networks and our generated networks, and compare their distributions. For consistency, we treat all networks as undirected. Since the number of nodes varies across networks, we focus on network metrics that are comparable across graphs of different sizes, and scale those that are dependent on network size based on how they are expected to scale in an Erdős-Rényi random graph (Erdős and Rényi, 1959). Below, we define and motivate the network metrics that we evaluate on.

Density. A basic property of a network is its density of edges, and social networks tend to be sparse, meaning lower density (Wong et al., 2006). Density computed as the number of observed edges

²<http://www.casos.cs.cmu.edu/tools/datasets/external/index.php>

³<http://konect.uni-koblenz.de/networks/>

divided by the total number of possible edges in the network, which comes out to $\frac{2E}{N(N-1)}$, where N is the number of nodes and E is the number of edges in the network.

Average clustering coefficient. Social networks are known to exhibit clustering, where one’s friends are likely to be friends with each other (Alizadeh, 2017). For a node i , its clustering coefficient is $\frac{2E_i}{N_i(N_i-1)}$, where N_i is its number of neighbors and E_i is the number of edges between its neighbors. The average clustering coefficient computes the average over nodes.

Proportion of nodes in the largest connected component (LCC). Social networks are known to be well-connected (Ugander et al., 2011), with the vast majority (over 99%) of the nodes in the largest connected component (LCC), i.e., the largest subgraph where all nodes within the subgraph are reachable by each other. Thus, as a metric, we compute the proportion of all nodes in the network that are in the LCC, $\frac{N_{LCC}}{N}$.

Average shortest path in LCC. Social networks are not only well-connected, meaning nodes can reach each other, but also they can reach each other in relatively short paths (Watts and Strogatz, 1998; Alizadeh, 2017). So, we measure the average shortest path over all pairs of nodes in the LCC, divided by $\log N_{LCC}$, since shortest paths scale with $\log N$ in Erdős-Rényi graphs (Watts and Strogatz, 1998). We compute shortest paths within the LCC instead of the entire network, since the distance between two disconnected nodes is infinite.

Community structure. Social networks exhibit strong community structure, with more edges within communities and fewer edges across communities (Newman, 2004). To measure community structure, first we use the Louvain algorithm (Blondel et al., 2008) to partition the network into communities, then we assess the quality of the partition with modularity (Eq. 3). Higher levels of community structure correspond to higher modularity.

Degree distribution. Social networks are said to follow a power law degree distribution, where $P(k) \sim k^{-\gamma}$, for degree k and constant γ (Barabási and Albert, 1999). This results in long-tailed degree distributions with a few people having far more friends than most others. To measure degree distribution, we compute the degree of each node in the network, and to make degree comparable

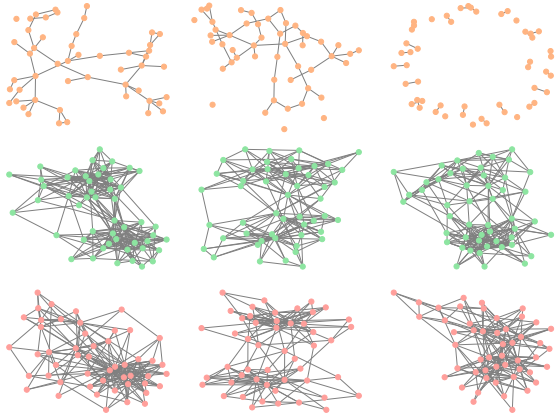


Figure 2: Generated social networks from different prompting methods: Global (top), Local (middle), Sequential (bottom).

across graphs, we divide degree by N . To summarize degree distribution from a set of networks (e.g., all real networks), we pool all of the (normalized) degrees of the nodes in the networks in the set, and compute the distribution over the pooled degrees in bins of 0.05 (from 0 to 1).

Homophily. Finally, social networks are known to exhibit homophily, where “birds of a feather flock together”, i.e., people with similar traits are likelier to be friends (McPherson et al., 2001; Kossinets and Watts, 2009). To measure homophily, we consider the observed proportion of same-group edges (e.g., same gender), divided by the expected proportion of same-group edges, given the number of nodes in each group:

$$H = \frac{S_{\text{obs}}}{S_{\text{exp}}} = \frac{\sum_{ij} A_{ij} \cdot \mathbb{1}[g_i = g_j]}{\frac{E}{\sum_g N_g(N_g - 1)}}, \quad (1)$$

where A_{ij} , as the adjacency matrix, is 1 if nodes i and j are connected and 0 otherwise; g_i indicates node i ’s group; and N_g is the number of nodes in group g . Higher ratios (above 1) indicate homophily and lower ratios (below 1) indicate heterophily, meaning there are fewer same-group relations than expected (this appears, for example, in heterosexual dating networks).

5 Results

Experimental set-up. We experiment with the following LLMs: OpenAI’s GPT-3.5 Turbo and GPT-4o (Brown et al., 2020; OpenAI et al., 2023), Meta’s Llama 3.1 (8B and 70B) (Touvron et al., 2023), and Google’s Gemma 2 (9B and 27B)

(Gemma Team et al., 2024), representing a range of models across companies and sizes. We find that GPT-3.5 Turbo performs the best at matching the real social networks, so we report results from GPT-3.5 Turbo in the main text, but we report results from all models in Appendix A. We show that our main results about political homophily being most emphasized and overestimated hold for all six models. We also include sensitivity analyses, with different temperatures (Figure 13) and minor changes to the prompt (Figure 14), and show that results are stable.

We sample $N = 50$ personas and we use the same set of personas for all LLM experiments. In Table 7, we report the demographic make-up of these 50 sampled personas. For each prompting method, we generate 30 networks, to capture variation in prompting (e.g., order of personas) and model response. For the graph-level metrics, we visualize their mean and standard error, along with individual data points (Figures 3 and 5). Visualizing both the standard error and individual data points capture inferential uncertainty and outcome variability, as recommended by Zhang et al. (2023).

5.1 Evaluating network structure

Here, we describe our main results from evaluating the structure of the generated networks.

Local and Sequential are more realistic than Global. First, we find that the prompting methods produce visually different network structures, as shown in Figure 2. Furthermore, the networks produced by the Global method are far less realistic than those produced by Local and Sequential. As shown in Figures 3-4, Global has unrealistically low density, clustering, and connectivity, too much community structure, and misses the long tail of the degree distribution. In comparison, Local and Sequential overlap with the real distributions for all graph-level metrics and show much greater variation in node degrees.

Thus, LLMs produce more realistic social networks when we assign the LLM to act as one persona at a time, instead of prompting it to produce the entire network at once. This is interesting, since the LLM has strictly less information under the one-persona setting: in the Local setting, it has no access to any network information, only making local decisions per persona based on demographics, and in the Sequential setting, it only knows the network based on previous personas’ choices

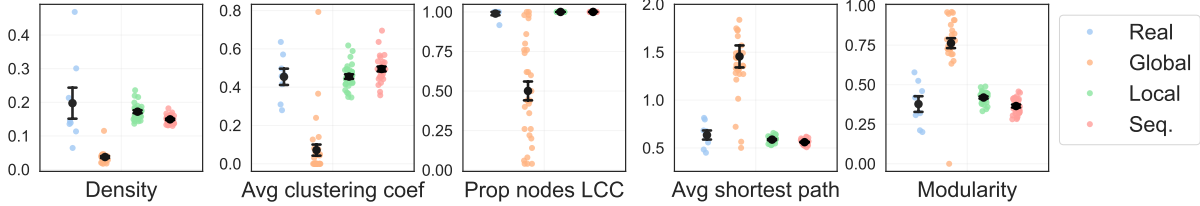


Figure 3: Graph-level metrics over real and generated social networks. We visualize mean and standard error (in black) and individual data points corresponding to each network.

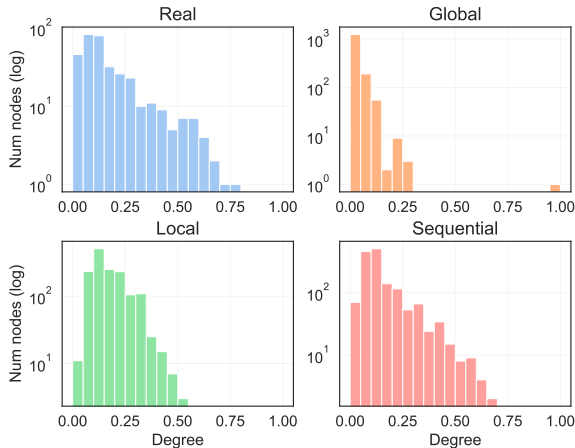


Figure 4: Degree distributions over real and generated social networks. For each set of networks, we pool degrees over nodes in the networks (Section 4).

without any ability to see into the future. In comparison, the Global method allows the LLM to take into account the entire network at once, along with all personas’ demographic information, so that it can theoretically consider dependencies between all these pieces of information. However, the LLM appears overwhelmed instead by the level of information, and produces far less realistic networks.

Sequential captures long-tail degree distribution.

By comparing Local and Sequential, we can isolate the impact of incorporating network information, on top of providing demographic information. The main difference between the two methods is the degree distribution: as shown in Figure 4, Sequential gets much closer to the real degree distribution, in terms of exhibiting a long tail, while Local approximately matches the mode without matching the tail. We also find that Sequential exhibits slightly less community structure and less homophily than Local, which makes sense since Local only matches on demographic similarity while Sequential also takes into account network information.

Thus, the Sequential method is able to match

real social networks on many structural characteristics. In Table 3, we quantify how well each LLM method matches the real networks, and compare to classical network models, including random graph models (Erdős and Rényi, 1959), small-world models (Watts and Strogatz, 1998), and preferential attachment models (Barabási and Albert, 1999). Even in the best case—when we allow the classical models to choose parameters based on the real networks—these models cannot match all of the characteristics as well as our Local or Sequential methods can. For example, when using the Kolmogorov-Smirnov statistic (Eq. 5) to measure distance between distributions, Sequential achieves an average distance of 0.330, while the best classical model (small-world) yields an average distance of 0.499, 51% higher than Sequential.

5.2 Evaluating homophily

We measure homophily for gender, race/ethnicity, religion, and political affiliation, using the ratio of observed-to-expected same-group relations (1).⁴

LLMs capture homophily, with greatest emphasis on politics.

In Figure 5, we show that, across all prompting methods and demographic variables, the generated networks clearly exhibit homophily. Furthermore, we see different levels of homophily for different demographic variables. For the more realistic Local and Sequential methods, homophily is by far the strongest for political affiliation: observed same-party relations are 85% more frequent than expected under Local and 68% more frequent than expected under Sequential. Rates of political homophily are even higher for the five other LLMs that we test, most extremely for GPT-4o and Llama 3.1 70B, where 100% of edges are same-party and the network fractures into two disconnected components (Appendix A).

⁴We cannot evaluate age homophily using Eq. 1, since “same-group” is ill-defined for a numerical variable like age, but we show in Appendix B that there is clear age homophily in the generated networks (Figure 10).

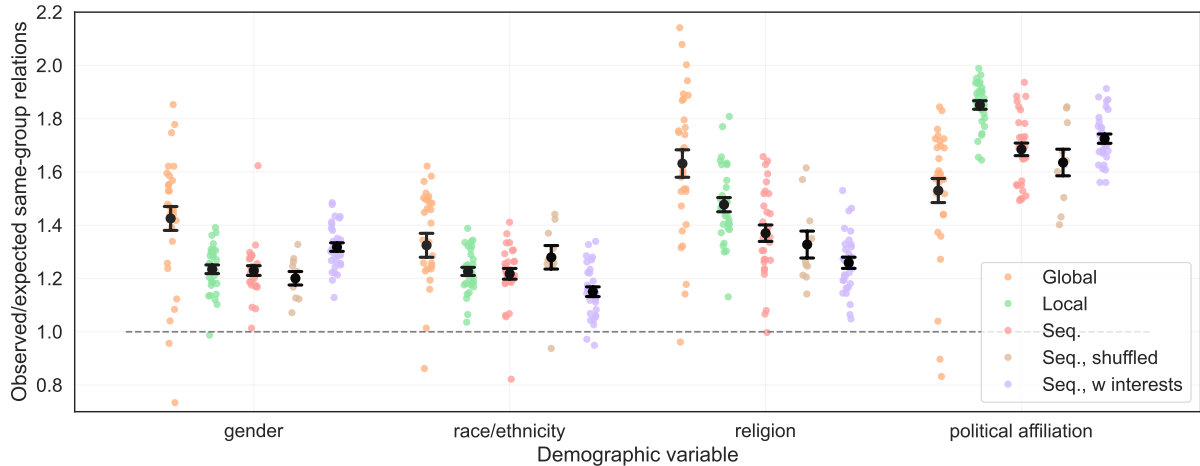


Figure 5: Rates of homophily in our generated networks, per demographic variable. Ratios above 1 (marked by the grey line) indicate homophily, with higher ratios indicating more homophily.

Does this mean that LLMs actually pay the most attention to political affiliation when choosing social ties? Despite political homophily being the strongest, this could be due to correlations between political affiliation and other demographics; for example, hypothetically, if all Democrats had the same gender and race, and all Republicans had the same gender and race, then apparent homophily in political affiliation could actually be due to similarity in other demographics. To test this, we try shuffling the demographics, so that, while maintaining the same numbers of each group per demographic, each persona is randomly assigned to a group, thus removing correlations between demographics. When we run Sequential with these shuffled personas, we find that political homophily remains by far the strongest, 30 points above the next demographic variable (Figure 5), demonstrating that the LLM is, in fact, paying most attention to political affiliation when choosing social ties. We also test this hypothesis directly by prompting the LLM to generate a short reason for each friend that it selects. Similar politics is mentioned 87% of the time, while the next most-mentioned demographic variable, religion, is only mentioned 43% of the time (details in Appendix B).

LLMs overestimate political homophily. Given the LLM’s emphasis on political homophily, we seek to compare its level of political homophily to reported levels from real-world social networks. We are not able to compare to the eight social networks from Section 5.1 here since we do not have demographic features per node. However, we are able to find reported political homophily in sev-

eral papers, covering both online and offline social networks. In Table 1, we summarize these comparisons, showing that Local and Sequential consistently overestimate political homophily across different measures of homophily.

For example, Halberstam and Knight (2016) analyze political homophily on Twitter. In their data, same-party relations only appear 40.4% more often than expected, significantly lower than what the LLM predicts. They also compute the isolation index, which is the difference in average conservative exposure between conservatives and liberals (Eq. 6), with larger indices indicating greater isolation. They find an isolation index of 0.403, while the LLM’s is far higher, at 0.720 for Local and 0.530 for Sequential. Furthermore, the authors note that homophily could be overestimated in their data, since they selected users who follow politicians, which “may tend to disproportionately include individuals with strong preferences for linking to like-minded users.” Even though their homophily results could be overestimates, the LLM’s estimates still significantly exceed theirs.

Isolation indices are even lower in Gentzkow and Shapiro (2011), who study ideological segregation in social networks. In face-to-face interactions, the highest isolation indices they report are 0.243 (family), 0.303 (people you trust) and 0.394 (among people who discuss politics). Finally, we also compare to Garimella and Weber (2017), who study political polarization on Twitter and define it as $p_i = 2 \cdot |0.5 - \alpha / (\alpha + \beta)|$, where α and β indicate how many left-leaning and right-leaning users, respectively, are followed by user i , and they take

Measure	Local	Sequential	Source	Description	Value
Same-group ratio (Eq. 1)	1.851 (0.016)	1.685 (0.024)	Halberstam and Knight (2016)	Twitter	1.404
Isolation index (Eq. 6)	0.720 (0.020)	0.530 (0.027)	Halberstam and Knight (2016) Gentzkow and Shapiro (2011)	Twitter	0.403
				Voluntary associations	0.145
				Work	0.168
				Neighborhood	0.187
				Family	0.243
Polarization (Eq. 7)	0.639 (0.037)	0.515 (0.041)	Garimella and Weber (2017)	People you trust	0.303
				Political discussants	0.394
				Twitter, follow	0.33-0.42
				Twitter, retweet	0.37-0.41

Table 1: Comparing political homophily in our generated networks to real-world networks. For Local and Sequential, we report the mean and standard error (in parentheses) over each method’s 30 generated networks.

the average p_i over users (Eq. 7). Their measure captures the difference between observed leaning and a balanced leaning of 0.5, with higher numbers indicating greater polarization. Using this measure, we find polarization levels of 0.639 for Local and 0.515 for Sequential, while Garimella and Weber (2017) report substantially lower numbers, with 0.33-0.42 for follows and 0.37-0.41 for retweets.

We hypothesize that the LLM overestimates political homophily partially due to high levels of polarization in its online pretraining data and frequent discussions of such polarization, although future work is needed to carefully study this phenomena. These results also have important implications if one seeks to run experiments over social networks generated by LLMs. For example, overestimated political homophily may result in unrealistically high levels of polarization, potentially leading to incorrect conclusions and interventions.

5.3 Incorporating interests

A natural question is whether demographic homophily is exaggerated because we only give the LLM demographic information, without other important details such as the person’s interests. Thus, we run an additional set of experiments where we allow the LLM to also generate interests for each persona. To generate interests, we prompt the LLM with, “In 8-12 words, describe the interests of someone with the following demographics” (full prompt in Figure 16). In Table 2, we provide examples of the generated interests, with the full list of personas with interests available online.

Effect of interests on networks. As shown in Figure 5, by comparing Sequential vs. Sequential with interests, we find that incorporating in-

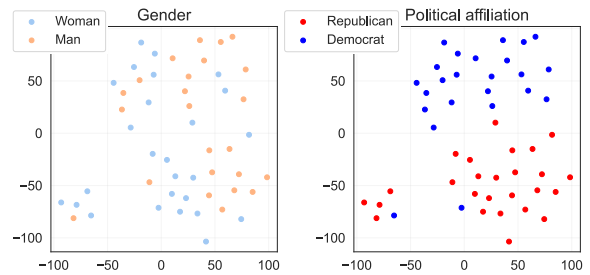


Figure 6: Embeddings of interests, with T-SNE projection to 2D. Each dot is a persona, colored by its gender (left) or its political affiliation (right).

terests increases homophily for some demographics (clearly for gender and slightly for political affiliation) and decreases homophily for the others (race/ethnicity and religion). Notably, after these adjustments, political homophily remains the strongest across the demographic variables. Thus, our finding that LLMs prioritize political homophily is robust to incorporating interests.

In fact, the interests themselves strongly encode political homophily, with evidence of political stereotyping. For example, among the Democrat personas, the most common interests are “social justice” (62.5% of Democrats vs. 0.2% of Republicans), “community service” (29.3% vs 13.9%), and “progressive policies” (18.6% vs. 0%). In contrast, among the Republican personas, the most common interests are “conservative politics” (41.6% of Republicans vs. 0% of Democrats), “church activities” (32.1% vs 13.2%), and “gardening” (23.2% vs 16.4%). We provide the complete list of top 10 interests per group in Table 5.

We also analyze interests by mapping them to text embeddings, using OpenAI’s text-embedding-3-small model. In Figure 6, we visualize the embed-

Gender	Race / Ethnicity	Age	Religion	Political Affiliation	Interests
Man	White	47	Protestant	Republican	Hunting, fishing, classic rock, church activities, patriotic events, home improvement
Woman	Black	69	Unreligious	Republican	History, gardening, community service, classic jazz music, financial news, travel
Man	Hispanic	75	Unreligious	Democrat	Historical documentaries, community events, family gatherings, literature on social justice
Man	American Indian / Alaska Native	30	Protestant	Republican	Outdoor activities, traditional crafts, conservative politics, music, community service, history
Woman	Asian	58	Catholic	Democrat	Volunteering, social justice, culinary arts, family activities, church community involvement

Table 2: Examples of LLM-generated interests for personas with different demographics.

dings, coloring them by their persona’s gender (left) and political affiliation (right). We compare these two demographic variables, since both have two, approximately equally sized groups in our sample of 50 personas. From this comparison, we can see how much more distinct the political groups are than the gender groups, demonstrating the level of political homophily encoded in the interests. Finally, we conduct a supplementary experiment where we try network generation with *only* interests and no demographics. As expected, homophily decreases across all demographic variables, but political homophily remains the strongest, 20 points above the next demographic variable (Figure 12).

These results demonstrate how the LLM’s emphasis on political affiliation also appears in interest generation, and, as a result, incorporating LLM-generated interests cannot help to reduce overestimated political homophily. These results build on prior results showing that LLM sometimes exhibit bias in political settings (Cheng et al., 2023b; Santurkar et al., 2023; Wang et al., 2024), exploring these issues through a novel lens of homophily and social network generation.

6 Discussion

Our work has established several findings. First, “local” prompting methods result in more realistic social networks than “global” methods, even though local settings receive less information about the existing network. Second, within local methods, adding network information (i.e., Sequential) helps the LLM produce more realistic networks, so that long-tailed degree distributions are captured. Third, the LLM clearly exhibits homophily across five key demographic variables, but political homophily dominates, to the extent that it is overestimated relative to real-world measures. Finally, incorporating LLM-generated interests does not re-

duce these overestimates, since the interests themselves encode strong political homophily.

Our findings demonstrate the promise of generating social networks with LLMs, as they are zero-shot, flexible, and able to simultaneously match many structural characteristics of real social networks. However, more needs to be done to address potential biases in social network generation with LLMs, especially with regards to political homophily. There are also other limitations to LLM social network generation: for example, while we have shown that Sequential can approximately match the *means* of the real networks’ metrics, its generated networks consistently demonstrate less *variance* than the real networks (Figure 3), reflecting known issues of LLMs to flatten demographic groups (Wang et al., 2024) and lack output diversity (Kirk et al., 2023). Furthermore, all of our methods require listing N personas per prompt, which becomes infeasible with larger networks, due to context windows and cost. In Table 6, we conduct a big-O analysis of how the number of tokens scales with network size, revealing a tradeoff between the improved realism of Sequential and Local versus the lower costs of Global.

In future work, we hope to develop LLM network generation methods that can balance realism and costs, as well as generate networks with greater variance. We also hope to explore methods to mitigate the political bias in generated networks. Instead of LLM-generated interests, researchers could handcraft interests with fewer political stereotypes, although other methods would be needed to scale such efforts for large social networks. We also discuss in the Appendix that the LLM’s emphasis on political homophily seems to come at the cost of underestimating other types of homophily, especially for race/ethnicity, and we hope to investigate homophily along these other dimensions more systematically in future work.

Acknowledgments

We thank Joon Sung Park and Marios Papachristou for helpful comments. S.C. was supported in part by a Meta PhD Fellowship and NSF Graduate Research Fellowship. We also gratefully acknowledge the support of NSF under Nos. OAC-1835598 (CINES), CCF-1918940 (Expeditions), DMS-2327709 (IHBEM); Stanford Data Applications Initiative, Wu Tsai Neurosciences Institute, Stanford Institute for Human-Centered AI, Chan Zuckerberg Initiative, Amazon, Genentech, GSK, Hitachi, SAP, and UCB.

References

- Chirag Agarwal, Sree Harsha Tanneru, and Himabindu Lakkaraju. 2024. Faithfulness vs. plausibility: On the (un)reliability of explanations from large language models. *arXiv preprint arXiv:2402.04614*.
- Gati Aher, Rosa I. Arriaga, and Adam Tauman Kalai. 2023. Using large language models to simulate multiple humans and replicate human subject studies. In *Proceedings of the 40th International Conference on Machine Learning (ICML'23)*.
- Meysam Alizadeh. 2017. Generating and analyzing spatial social networks. *Computational and Mathematical Organization Theory*, 23:362–390.
- Lisa P. Argyle, Ethan C. Busby, Nancy Fulda, Joshua R. Gubler, Christopher Rytting, and David Wingate. 2023. Out of one, many: Using language models to simulate human samples. *Political Analysis*, 31(3):337–351.
- Albert-László Barabási and Réka Albert. 1999. Emergence of scaling in random networks. *Science*, 286(5439):509–512.
- Christopher L. Barrett, Richard J. Beckman, Maleq Khan, V. S. Anil Kumar, Madhav V. Marathe, Paula E. Stretz, Tridib Dutta, and Bryan Lewis. 2009. Generation and analysis of large synthetic social contact networks. In *Proceedings of the 2009 Winter Simulation Conference (WSC'09)*, pages 1003–1014.
- Per Block, Marion Hoffman, Isabel J. Raabe, Jennifer Beam Dowd, Charles Rahal, Ridhi Kashyap, and Melinda C. Mills. 2020. Social network-based distancing strategies to flatten the COVID-19 curve in a post-lockdown world. *Nature Human Behaviour*, 4:588–596.
- Vincent D Blondel, Jean-Loup Guillaume, Renaud Lambiotte, and Etienne Lefebvre. 2008. Fast unfolding of communities in large networks. *Journal of statistical mechanics: theory and experiment*, 2008(10):P10008.
- Anna Brown. 2022. About 5% of young adults in the u.s. say their gender is different from their sex assigned at birth. *Pew Research Center*. <https://pewrsr.ch/3Qi2Ejd>.
- Tom B. Brown, Benjamin Mann, Nick Ryder, Melanie Subbiah, Jared Kaplan, Prafulla Dhariwal, Arvind Neelakantan, Pranav Shyam, Girish Sastry, et al. 2020. Language models are few-shot learners. *arXiv preprint arXiv:2005.14165*.
- Zhikai Chen, Haitao Mao, Hang Li, Wei Jin, Hongzhi Wen, Xiaochi Wei, Shuaiqiang Wang, Dawei Yin, Wenqi Fan, Hui Liu, et al. 2024. Exploring the potential of large language models (LLMs) in learning on graphs. *ACM SIGKDD Explorations Newsletter*, 25(2):42–61.
- Myra Cheng, Esin Durmus, and Dan Jurafsky. 2023a. Marked personas: Using natural language prompts to measure stereotypes in language models. In *Proceedings of the 61st Annual Meeting of the Association for Computational Linguistics (ACL'23)*, pages 1504–1532.
- Myra Cheng, Tiziano Piccardi, and Diyi Yang. 2023b. CoMPosT: Characterizing and evaluating caricature in LLM simulations. In *Proceedings of the 2023 Conference on Empirical Methods in Natural Language Processing (EMNLP'23)*, pages 10853–10875.
- Yun-Shiuan Chuang, Agam Goyal, Nikunj Harlalka, Siddharth Suresh, Robert Hawkins, Sijia Yang, Dhavan Shah, Junjie Hu, and Timothy T Rogers. 2023. Simulating opinion dynamics with networks of LLM-based agents. *arXiv preprint arXiv:2311.09618*.
- James Coleman, Elihu Katz, and Herbert Menzel. 1957. The diffusion of an innovation among physicians. *Sociometry*, 20(4):253–270.
- Pranav Dandekar, Ashish Goel, and David T. Lee. 2013. Biased assimilation, homophily, and the dynamics of polarization. *Proceedings of the National Academy of Sciences (PNAS)*, 110(15):5791–5796.
- Abhimanyu Das, Sreenivas Gollapudi, and Kamesh Munagala. 2014. Modeling opinion dynamics in social networks. In *Proceedings of the 7th ACM international conference on Web search and data mining (WSDM'14)*, pages 403–412.
- Ameet Deshpande, Vishvak Murahari, Tanmay Rajpurohit, Ashwin Kalyan, and Karthik Narasimhan. 2023. Toxicity in chatgpt: Analyzing persona-assigned language models. In *Findings of the Association for Computational Linguistics: EMNLP 2023*, pages 1236–1270.
- Paul Erdős and Alfréd Rényi. 1959. On random graphs i. *Publicationes Mathematicae Debrecen*, 6:290–297.
- Bahare Fatemi, Jonathan Halcrow, and Bryan Perozzi. 2024. Talk like a graph: Encoding graphs for large language models. In *Proceedings of the 12th International Conference on Learning Representations (ICLR'24)*.

- Chen Gao, Xiaochong Lan, Zhihong Lu, Jinzhu Mao, Jinghua Piao, Huandong Wang, Depeng Jin, and Yong Li. 2023. Social-network simulation system with large language model-empowered agents. *arXiv preprint arXiv:2307.14984*.
- Kiran Garimella and Ingmar Weber. 2017. A long-term analysis of polarization on twitter. In *ICWSM'17: Proceedings of the International AAAI Conference on Web and Social Media*, volume 11, pages 528–531.
- Gemma Team, Thomas Mesnard, Cassidy Hardin, Robert Dadashi, Surya Bhupatiraju, Shreya Pathak, Laurent Sifre, Morgane Rivière, Mihir Sanjay Kale, Juliette Love, Pouya Tafti, et al. 2024. Gemma: Open models based on gemini research and technology. *arXiv preprint arXiv:2403.08295*.
- Matthew Gentzkow and Jesse M. Shapiro. 2011. Ideological segregation online and offline. *The Quarterly Journal of Economics*, 126:1799–1839.
- Xiaojie Guo and Liang Zhao. 2023. A systematic survey on deep generative models for graph generation. *IEEE Transactions on Pattern Analysis and Machine Intelligence*, 45(5):5370–5390.
- Shashank Gupta, Vaishnavi Shrivastava, Ashwin Kalyan Ameet Deshpande, Peter Clark, Ashish Sabharwal, and Tushar Khot. 2024. Bias runs deep: Implicit reasoning biases in persona-assigned LLMs. In *Proceedings of the 12th International Conference on Learning Representations (ICLR'24)*.
- Yosh Halberstam and Brian Knight. 2016. Homophily, group size, and the diffusion of political information in social networks: Evidence from twitter. *Journal of Public Economics*, 143:73–88.
- Jochen Hartmann, Jasper Schwenzow, and Maximilian Witte. 2023. The political ideology of conversational AI: Converging evidence on ChatGPT’s pro-environmental, left-libertarian orientation. *arXiv preprint arXiv:2301.01768*.
- James He, Felix Wallis, Andrés Gvartz, and Steve Rathje. 2023. Artificial intelligence chatbots mimic human collective behaviour. *Research Square*.
- Joseph Lawson Hodges Jr. 1958. The significance probability of the Smirnov two-sample test. *Arkiv fiur Matematik*, 3(43):469–486.
- Paul W Holland, Kathryn Blackmond Laskey, and Samuel Leinhardt. 1983. Stochastic blockmodels: First steps. *Social Networks*, 5(2):109–137.
- Bowen Jin, Gang Liu, Chi Han, Meng Jiang, Heng Ji, and Jiawei Han. 2024. Large language models on graphs: A comprehensive survey. *arXiv preprint arXiv:2312.02783*.
- Bruce Kapferer. 1972. *Strategy and transaction in an African factory*. Manchester University Press, Manchester.
- Robert Kirk, Ishita Mediratta, Christoforos Nalmpantis, Jelena Luketina, Eric Hambro, Edward Grefenstette, and Roberta Raileanu. 2023. Understanding the effects of RLHF on LLM generalisation and diversity. *arXiv preprint arXiv:2310.06452*.
- Gueorgi Kossinets and Duncan J. Watts. 2009. Origins of homophily in an evolving social network. *American Journal of Sociology*, 115(2).
- David Krackhardt. 1999. The ties that torture: Simmelian tie analysis in organizations. *Research in the Sociology of Organizations*, 16:183–210.
- Yuhan Li, Zhixun Li, Peisong Wang, Jia Li, Xiangguo Sun, Hong Cheng, and Jeffrey Xu Yu. 2024. A survey of graph meets large language model: Progress and future directions. In *Proceedings of the Thirty-Third International Joint Conference on Artificial Intelligence (IJCAI'24)*.
- Duncan MacRae Jr. 1960. Direct factor analysis of sociometric data. *Sociometry*, 23(4):360–371.
- Giordano De Marzo, Luciano Pietronero, and David Garcia. 2023. Emergence of scale-free networks in social interactions among large language models. *arXiv preprint arXiv:2312.06619*.
- Miller McPherson, Lynn Smith-Lovin, and James M Cook. 2001. Birds of a feather: Homophily in social networks. *Annual Review of Sociology*, 27(1):415–444.
- Mark E. J. Newman. 2004. Fast algorithm for detecting community structure in networks. *Phys. Rev. E*, 69:066133.
- OpenAI, Josh Achiam, Steven Adler, Sandhini Agarwal, Lama Ahmad, Ilge Akkaya, Florencia Leoni Aleman, Diogo Almeida, Janko Altschmidt, Sam Altman, et al. 2023. GPT-4 technical report. *arXiv preprint arXiv:2303.08774*.
- Shirui Pan, Linhao Luo, Yufei Wang, Chen Chen, Jipu Wang, and Xindong Wu. 2024. Unifying large language models and knowledge graphs: A roadmap. *IEEE Transactions on Knowledge and Data Engineering*, 36(7):3580–3599.
- Marios Papachristou and Yuan Yuan. 2024. Network formation and dynamics among multi-LLMs. *arXiv preprint arXiv:2402.10659*.
- Joon Sung Park, Joseph O’Brien, Carrie Jun Cai, Meredith Ringel Morris, Percy Liang, and Michael S Bernstein. 2023. Generative agents: Interactive simulacra of human behavior. In *Proceedings of the 36th Annual ACM Symposium on User Interface Software and Technology (UIST'23)*, pages 1–22.
- Joon Sung Park, Lindsay Popowski, Carrie Cai, Meredith Ringel Morris, Percy Liang, and Michael S Bernstein. 2022. Social simulacra: Creating populated prototypes for social computing systems. In *Proceedings of the 35th Annual ACM Symposium on User Interface Software and Technology*, pages 1–18.

- Hebert Pérez-Rosés and Francesc Sebé. 2015. Synthetic generation of social network data with endorsements. *Journal of Simulation*, 9(4):279–286.
- Pew Research Center. 2024. Partisanship by race, ethnicity and education. <https://www.pewresearch.org/politics/2024/04/09/partisanship-by-race-ethnicity-and-education/#partisanship-by-race-and-gender>.
- PRRI Staff. 2021. 2020 PRRI census of American religion: County-level data on religious identity and diversity. <https://www.prrri.org/research/2020-census-of-american-religion/>.
- Yalin E. Sagduyu, Alexander Grushin, and Yi Shi. 2018. Synthetic social media data generation. *IEEE Transactions on Computational Social Systems*, 5(3):605–620.
- Gabriel R. Sanchez and Raymond Foxworth. 2022. Native americans support democrats over republicans across house and senate races. *Brookings*. <https://www.brookings.edu/articles/native-americans-support-democrats-over-republicans-across-house-and-senate-races/>.
- Shibani Santurkar, Esin Durmus, Faisal Ladhak, Cino Lee, Percy Liang, and Tatsunori Hashimoto. 2023. Whose opinions do language models reflect? In *Proceedings of the 40th International Conference on Machine Learning (ICML’23)*, pages 29971–30004.
- Martin Simonovsky and Nikos Komodakis. 2018. GraphVAE: Towards generation of small graphs using variational autoencoders. In *Artificial Neural Networks and Machine Learning–ICANN 2018: 27th International Conference on Artificial Neural Networks, Rhodes, Greece, October 4-7, 2018, Proceedings, Part I 27*, pages 412–422. Springer.
- Jeffrey A. Smith, Miller McPherson, and Lynn Smith-Lovin. 2014. Social distance in the United States: Sex, race, religion, age, and education homophily among confidants, 1985 to 2004. *American Sociological Review*, 79.
- Statista. 2016. Religious identity of adults in the United States in 2016, by race and ethnicity. <https://www.statista.com/statistics/749128/religious-identity-of-adults-in-the-us-by-race-and-ethnicity/>.
- Mike Thelwall. 2009. Homophily in myspace. *Journal of the American Society for Information Science and Technology*, 60(2):219–231.
- Hugo Touvron, Thibaut Lavril, Gautier Izacard, Xavier Martinet, Marie-Anne Lachaux, Timothée Lacroix, Baptiste Rozière, Naman Goyal, Eric Hambro, et al. 2023. LLaMA: Open and efficient foundation language models. *arXiv preprint arXiv:2302.13971*.
- Johan Ugander, Brian Karrer, Lars Backstrom, and Cameron Marlow. 2011. The anatomy of the Facebook social graph.
- US Census Bureau. 2023. National population by characteristics: 2020-2023. <https://www.census.gov/data/tables/time-series/demo/popest/2020s-national-detail.html>.
- Angelina Wang, Jamie Morgenstern, and John P. Dickerson. 2024. Large language models cannot replace human participants because they cannot portray identity groups. *arXiv preprint arXiv:2402.01908*.
- Heng Wang, Shangbin Feng, Tianxing He, Zhaoxuan Tan, Xiaochuang Han, and Yulia Tsvetkov. 2023. Can language models solve graph problems in natural language? In *Proceedings of the 37th Conference on Neural Information Processing Systems (NeurIPS 2023)*.
- Duncan J Watts and Steven H Strogatz. 1998. Collective dynamics of ‘small-world’ networks. *Nature*, 393(6684):440–442.
- Ling Heng Wong, Philippa Pattison, and Garry Robins. 2006. A spatial model for social networks. *Physica A: Statistical Mechanics and its Applications*, 360.
- Yang Yao, Xin Wang, Zeyang Zhang, Yijian Qin, Ziwei Zhang, Xu Chu, Yuekui Yang, Wenwu Zhu, and Hong Mei. 2024. Exploring the potential of large language models in graph generation. *arXiv preprint arXiv:2403.14358*.
- Ruosong Ye, Caiqi Zhang, Runhui Wang, Shuyuan Xu, and Yongfeng Zhang. 2024. Language is all a graph needs. In *Findings of the Association for Computational Linguistics: EACL 2024*, pages 1955–1973.
- Jiaxuan You, Rex Ying, Xiang Ren, William Hamilton, and Jure Leskovec. 2018. GraphRNN: Generating realistic graphs with deep auto-regressive models. In *Proceedings of the 35th International Conference on Machine Learning (ICML’18)*, pages 5708–5717.
- Wayne W. Zachary. 1977. An information flow model for conflict and fission in small groups. *Journal of Anthropological Research*, 33(4):452–473.
- Sam Zhang, Patrick R. Heck, Michelle N. Meyer, Christopher F. Chabris, Daniel G. Goldstein, and Jake Hofman. 2023. An illusion of predictability in scientific results: Even experts confuse inferential uncertainty and outcome variability. *Proceedings of the National Academy of Sciences (PNAS)*, 120(33).
- Jianan Zhao, Le Zhuo, Yikang Shen, Meng Qu, Kai Liu, Michael Bronstein, Zhaocheng Zhu, and Jian Tang. 2023. GraphText: Graph reasoning in text space. *arXiv preprint arXiv:2310.01089*.
- Xuhui Zhou, Hao Zhu, Leena Mathur, Ruohong Zhang, Haofei Yu, Zhengyang Qi, Louis-Philippe Morency, Yonatan Bisk, Daniel Fried, Graham Neubig, and Maarten Sap. 2024. SOTOPIA: Interactive evaluation for social intelligence in language agents. In *Proceedings of the 12th International Conference on Learning Representations (ICLR’24)*.

Appendix

In Appendix A, we compare results across GPT, Llama, and Gemma models. In Appendix B, we describe additional experiments and findings. In Appendix C, we provide details on methods and experimental set-up.

A Comparison between LLMs

We experiment with the following LLMs: OpenAI’s GPT-3.5 Turbo and GPT-4o (Brown et al., 2020; OpenAI et al., 2023), Meta’s Llama 3.1 (8B and 70B) (Touvron et al., 2023), and Google’s Gemma 2 (9B and 27B) (Gemma Team et al., 2024), representing a range of models across companies and sizes. For the OpenAI models, we use the OpenAI API,⁵ and for the other models, we use the Llama API,⁶ which also includes other open-source models. We report our main results on GPT-3.5 Turbo since we find that it best matches the structure of the real-world social networks (discussed below), but here, we discuss results from all other models. For these experiments, we generate networks with the Sequential method, using the same experimental settings as before (same set of 50 personas, prompt, temperature of 0.8, etc.). For these experiments, we generate 10 instead of 30 networks per model, but we find that standard errors are small. We visualize results for GPT-4o in Figure 7, Llama 3.1 8B and 70B in Figure 8, and Gemma 2 9B and 27B in Figure 9.

Structural characteristics. We find that GPT-3.5 Turbo best matches the structure of the real networks, most notably matching the real-world density. All of the other models have much higher densities, which also contributes to unrealistically high clustering and low shortest paths. Due to density’s outsized effect, we wanted to see if providing the model a bit of help on density might be all that it needs to match the other characteristics as well. Thus, we try a variant of the Sequential method where we specify n , i.e., how many friends should be chosen (instead of only asking “Which of these people will you become friends with?”, see full prompt in Figure 19). We sample n from Exponential($\lambda = 0.2$), with mean $1/\lambda = 5$, independently for each persona. Note that specifying each persona’s number of choices does not predetermine the exact density or degree distribution of

the network, since a persona’s total set of friends at the end of the network generating process is the union of its chosen friends along with anyone who chose it. However, specifying these numbers can help to guide the models to lower densities.

With this variant, which we call “ $+\lambda$ ”, all models’ densities are brought down to a reasonable range. Llama 3.1 8B $+\lambda$ is also able to approximately match the real networks and GPT-3.5 Turbo on all other characteristics now (Figure 8). However, even with $+\lambda$, GPT-4o and Llama 3.1 70B still generate networks that are often disconnected into two components; this is due to extreme political segregation, which we discuss below. With Gemma 2 27B, the networks are almost always fully connected, but even with $+\lambda$, clustering and modularity remain slightly too high.⁷

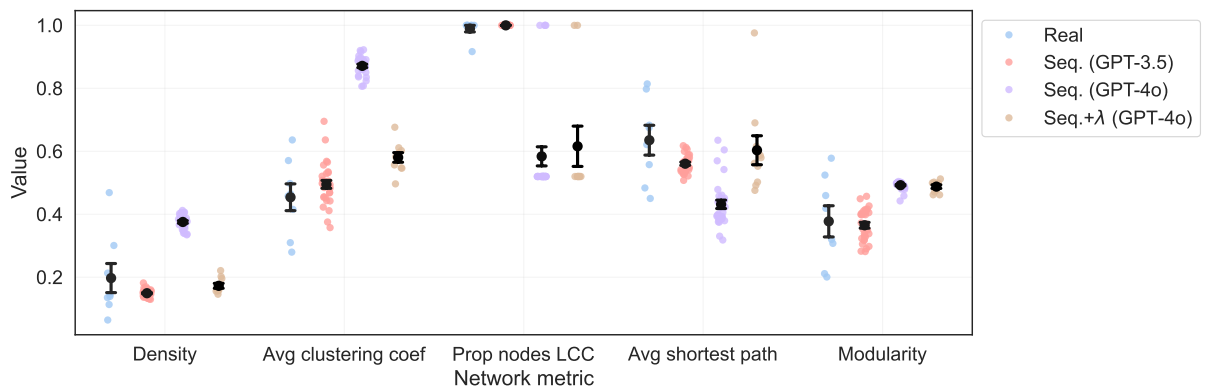
Homophily. We find that all six models exhibit clear homophily, with ratios above 1 for gender, race/ethnicity, religion, and political affiliation. We also find, consistently across the models, that political homophily remains by far the strongest, followed by religion, then race/ethnicity and gender. Political homophily is also always overestimated compared to real-world measures; in fact, the models we test in this section all produce levels of political homophily even higher than GPT-3.5 Turbo, which we discussed were overestimates in the main text (Table 1).

The emphasis on political homophily is particularly extreme for GPT-4o and Llama 3.1 70B: they show complete segregation between Republicans and Democrats, such that 100% of edges are same-group and political homophily reaches its maximum value. We can compute the maximum value based on the known numbers of nodes in each group: in our set of 50 sampled personas, we have 26 Republicans and 24 Democrats (Table 7). So, the expected proportion of same-group edges is $\frac{(26 \cdot 25) + (24 \cdot 23)}{50 \cdot 49} \approx 0.49$ (Eq. 1), so the maximum ratio is $1/0.49 \approx 2.04$, which is indeed the ratio that we see for GPT-4o and Llama 3.1 70B (with and without $+\lambda$). Furthermore, as a result of the complete segregation, their networks fracture into two disconnected components, one for Republicans and one for Democrats, which is why we see that the proportion of nodes in the largest connected component is often around 50% for these two models (Figure 7 and 8).

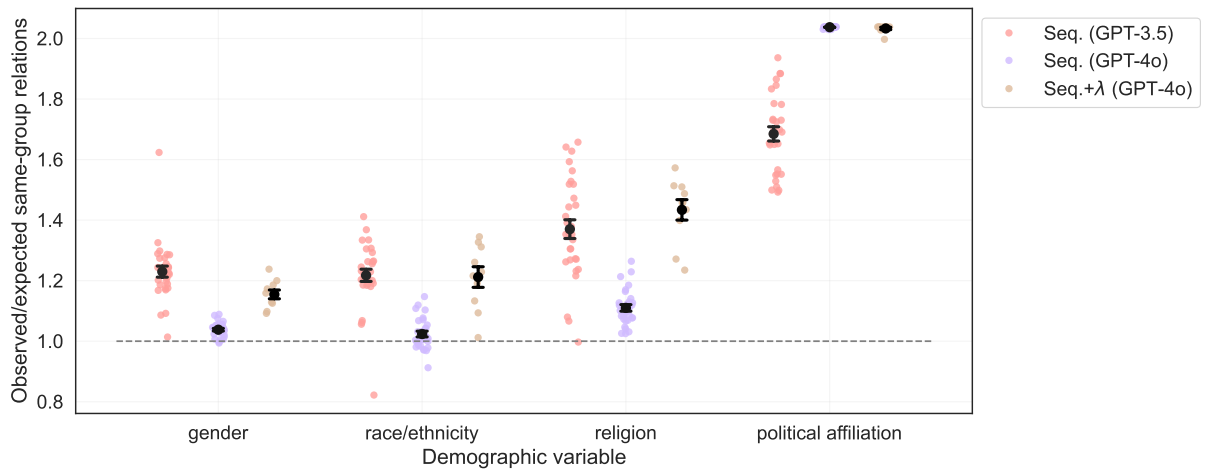
⁵<https://platform.openai.com/docs/api-reference>

⁶<https://www.llama-api.com/>

⁷We were not able to add $+\lambda$ to Gemma 2 9B, since it had trouble producing responses that exactly matched n .

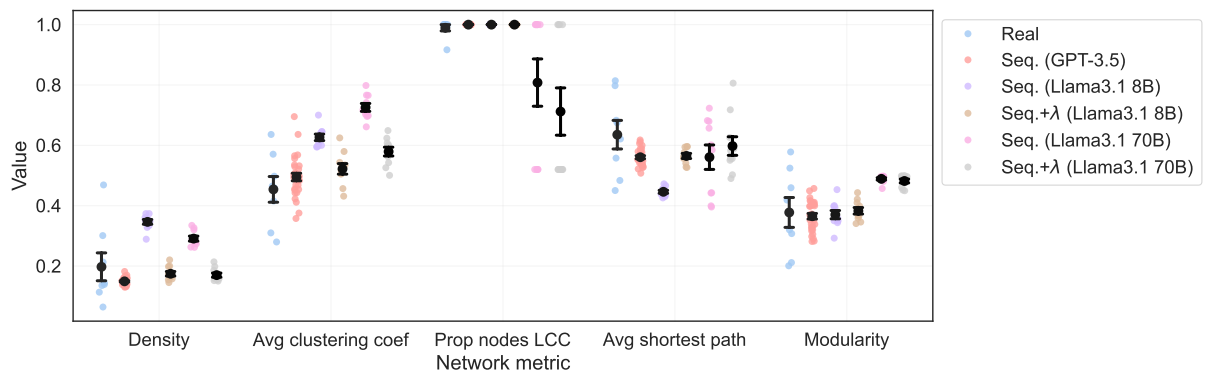


(a) Comparing structural network metrics.

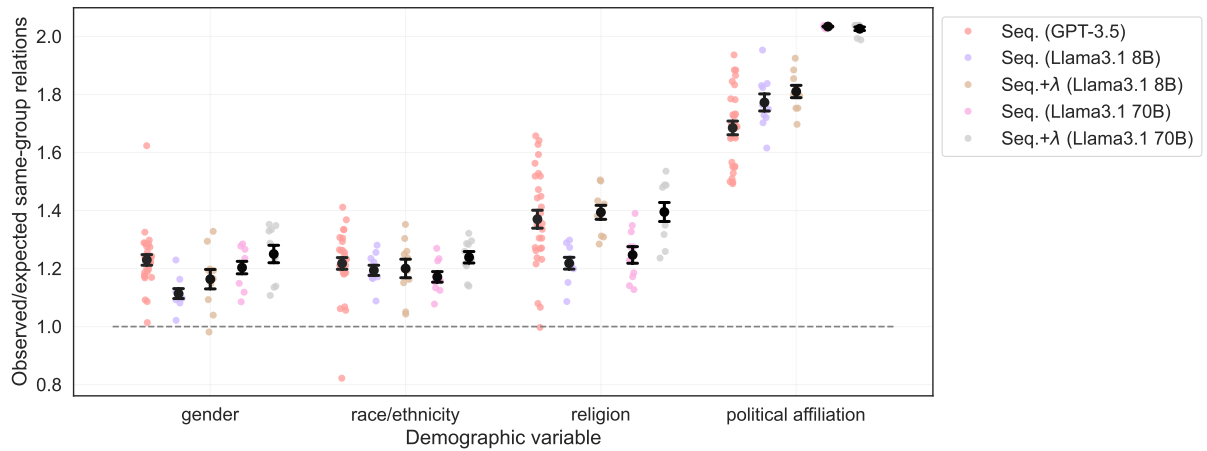


(b) Comparing homophily.

Figure 7: Evaluating results from GPT-4o, compared to GPT-3.5 Turbo.

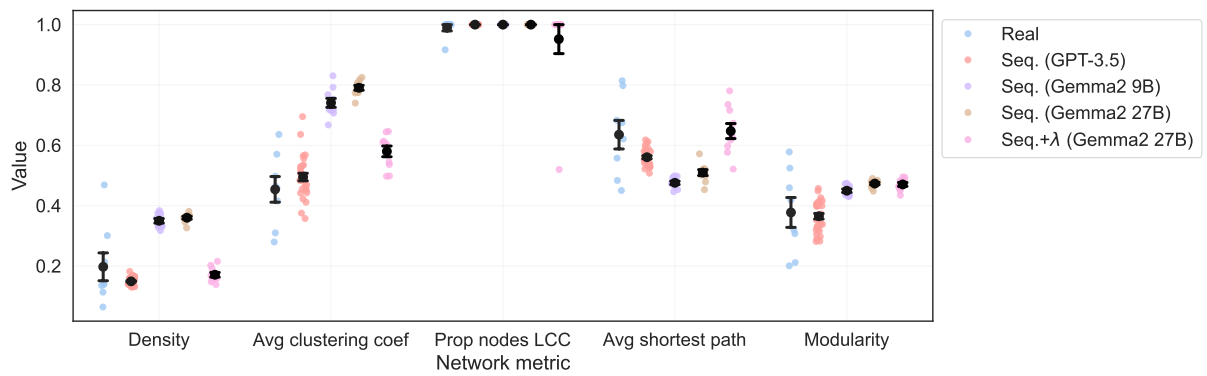


(a) Comparing structural network metrics.

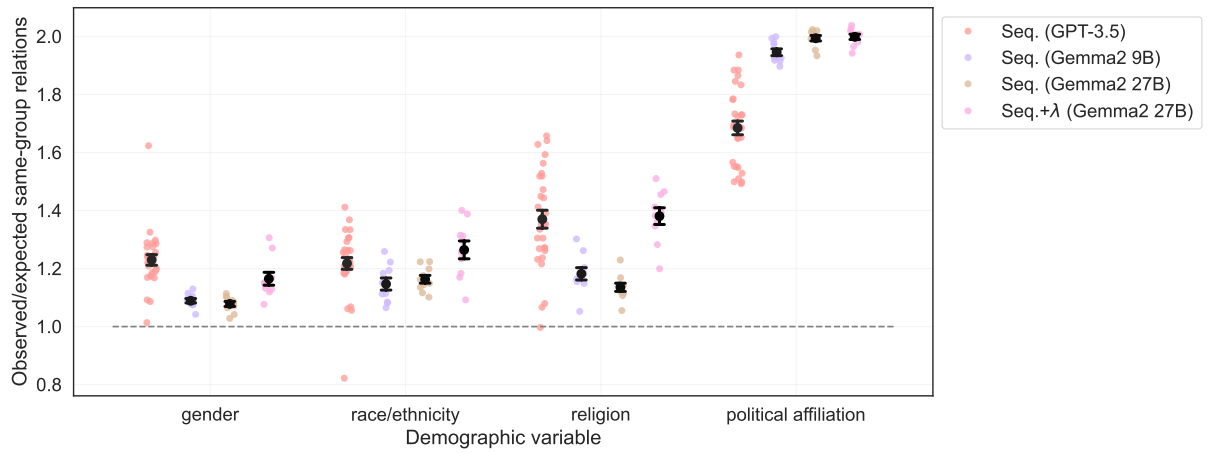


(b) Comparing homophily.

Figure 8: Evaluating results from Llama 3.1 8B and 70B, compared to GPT-3.5 Turbo.



(a) Comparing structural network metrics.



(b) Comparing homophily.

Figure 9: Evaluating results from Gemma 2 9B and 27B, compared to GPT-3.5 Turbo.

B Additional results

In this section, all experiments are run with GPT-3.5 Turbo, unless otherwise specified.

Comparing to classical network models. In the main text, we showed that the LLM can match many structural characteristics of real social networks, including density, clustering, connectivity, and degree distribution (Figures 3 and 4). However, how does this compare to existing models for network generation? Here, we consider three classical network models: (1) Erdős–Rényi random graph models (Erdős and Rényi, 1959), (2) Barabási–Albert preferential attachment models (Barabási and Albert, 1999), and (3) Watts–Strogatz small-world models (Watts and Strogatz, 1998). These models are close to zero-shot: they only require a 1-2 parameters to define, although we still need to fit these parameters. In contrast, we do not compare to stochastic block models (Holland et al., 1983), which require sizes per block and probabilities between each pair of blocks, or machine learning models for graph generation, since they have many parameters and require a substantial set of observed graphs for training to fit those parameters (You et al., 2018; Simonovsky and Komodakis, 2018; Guo and Zhao, 2023).

To quantify how well a network metric is matched, we extract the metric from each real social network, using the same eight social networks as in our main experiments (Sections 5.1 and C.3), and from each generated network, with 30 generated networks per model. To compare the two distributions of the metric, we report both the difference in the means, normalized by the real networks’ standard deviation (Eq. 4), and the two-sample Kolmogorov–Smirnov statistic (Eq. 5), which measures the distance between two empirical distributions. As we show in Table 3, even in the best case—when we allow the models to choose parameters based on the real social networks—these models cannot match all of the real network metrics as well as our Local or Sequential methods can. Thus, being able to match the structural characteristics of real social networks is non-trivial, adding significance to our finding that LLMs can match many structural characteristics at once.

Age homophily. We cannot directly apply our typical homophily measure, Eq. 1, to age, since it is not a categorical variable. However, we can still measure age homophily in a number of ways.

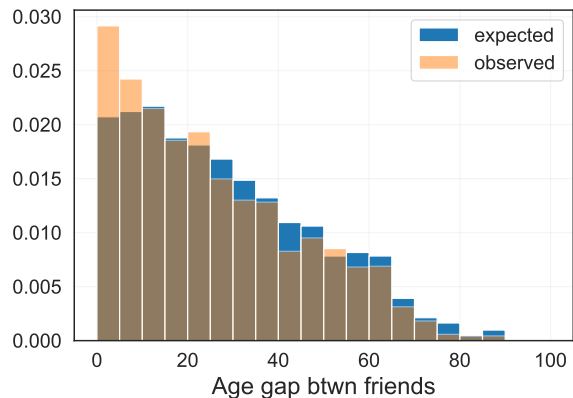


Figure 10: Observed (left) vs. expected (right) distribution of age gaps in the generated social networks, under the Sequential method.

First, we can replace $\mathbb{1}[g_i = g_j]$ with $\mathbb{1}[|age(i) - age(j)| \leq 10]$ in Eq. 1. Then, the ratio we are computing is the proportion of observed edges with an age gap less than or equal to 10, divided by the expected proportion of such edges. Note that ages range from 0 to 100 (Section C.1), so a gap of 10 is relatively small. Under this measure, we find values of 1.376 for Global, 1.254 for Local, and 1.258 for Sequential, indicating clear homophily. We can also plot the distribution of observed age gaps vs. expected age gaps, which we show in Figure 10. Compared to the expected distribution, the observed distribution is clearly shifted to the left (i.e., smaller gaps), with more edges than expected with age gaps of 0-10.

Reasons for choosing friends. We have seen under different models and prompts that political homophily is the strongest, out of the demographic variables that we test. We have also shown, after shuffling demographics to remove correlations between them, that the LLM still favors political homophily the most (Figure 5), suggesting that it is, in fact, paying the most attention to political affiliation when forming social relations. As another way to test this theory, we try directly asking the LLM to generate a short reason for each friend it selects. Then, given the reason, we use GPT-4o to classify the reason, e.g., “I’m a woman too and we share the same religion and political affiliation” is classified as [gender, religion, political affiliation]. We allow the LLM to generate free-text reasons during network generation since we do not want to constrain its response (e.g., if it is using other information, such as degree or ID).

We find that political affiliation strongly domi-

Model	Density	Avg CC	% LCC	Avg SP	Mod.	Degree	Avg
Random graph	0.013 [†]	2.286	0.378	1.156	1.149	0.154	1.025
Preferential attachment	0.113 [†]	1.363	0.378	1.081	1.160	0.053	0.807
Small world	0.054 [†]	0.041 [†]	0.378	0.808	0.404	0.188	0.444
GPT-3.5 Turbo, Global	1.311	3.399	17.740	6.547	2.959	0.914	5.478
GPT-3.5 Turbo, Local	0.207	0.012	0.378	0.383	0.316	0.023	0.220
GPT-3.5 Turbo, Sequential	0.394	0.363	0.378	0.596	0.088	0.174	0.332
Random graph	0.625	1.000	0.125	0.750	0.750	0.465	0.619
Preferential attachment	0.625	0.750	0.125	0.750	0.750	0.416	0.569
Small world	0.625	0.375	0.125	0.750	0.500	0.617	0.499
GPT-3.5 Turbo, Global	0.967	0.933	0.833	0.900	0.967	0.740	0.890
GPT-3.5 Turbo, Local	0.525	0.250	0.125	0.500	0.500	0.265	0.361
GPT-3.5 Turbo, Sequential	0.375	0.325	0.125	0.625	0.342	0.190	0.330

Table 3: Quantitative results on structural characteristics. The top six rows indicate difference in means, normalized by the real networks’ standard deviation (Eq. 4). [†] indicates that the model parameters were fitted on the real-world mean value for this characteristic, so the mean difference should be ignored, and it is left out of the average. The bottom six rows represent the two-sample Kolmogorov–Smirnov statistic, which measures the distance between two empirical distributions (Eq. 5). For both measures, lower is better.

Demographic	Reason %
Political affiliation	86.7%
Religion	43.0%
Age	21.8%
Race/ethnicity	12.1%
Gender	7.3%

Table 4: Frequency that each demographic is part of the reason given for choosing a persona as a friend.

notes here as well: it is part of the reason 86.7% of the time, while the next most-mentioned demographic, religion, is only mentioned 43.0% of the time (Table 4). As a caveat, note that we cannot always trust an LLM’s self-given reason or explanation for its choices (Agarwal et al., 2024). However, given the alignment of these results along with everything else we have seen, there is strong evidence that LLMs pay the most attention to political affiliation when generating social relations. We also test whether prompting the LLM to give a reason changes the structure of the generated networks. We show in Figure 14 that our main results do not significantly change, so they are robust to this modification in prompt.

Homophily between all pairs of groups. As described in the main text, we measure homophily as the ratio of observed same-group relations to expected same-group relations, based on the number of nodes in each group (Eq. 1). Now, we extend this definition to compute a measure for any pair

of groups, A and B (where A could equal B):

$$H_{AB} = \frac{\sum_{ij} A_{ij} \cdot \mathbb{1}[g_i=A] \cdot \mathbb{1}[g_j=B]}{\frac{N_A(N_B-1)[A=B]}{N(N-1)}}. \quad (2)$$

This measures the ratio of observed to expected edges for pair A, B . In Figure 11, we visualize H_{AB} for all pairs, for each of the four categorical demographic variables (gender, race/ethnicity, religion, and political affiliation). For each variable, we keep all groups with at least 3 personas in our set of 50 personas (Table 7), and compute H_{AB} for each pair of groups, reporting the mean ratio over the 30 generated networks from Sequential.

We find, as expected, that the diagonal (i.e., same-group relations) tends to be above 1, although notably it is not for relations between men, with a ratio of 0.99, while relations between women have a ratio of 1.43. Thus, even within one demographic variable, the LLM’s levels of homophily vary for different groups, such as homophily within women being stronger than homophily within men. Variability across groups is present for all demographic variables: most extremely, for race/ethnicity, relations between personas that identify as Black occur 3.44 \times more frequently than expected, the highest ratio we find, while overall homophily for race/ethnicity (following Eq. 1) is only 1.22. For political affiliation, both parties have strong same-group tendencies, with ratios of 1.54 and 1.85 for Republicans and Democrats, respectively, and a low cross-group ratio of 0.34.

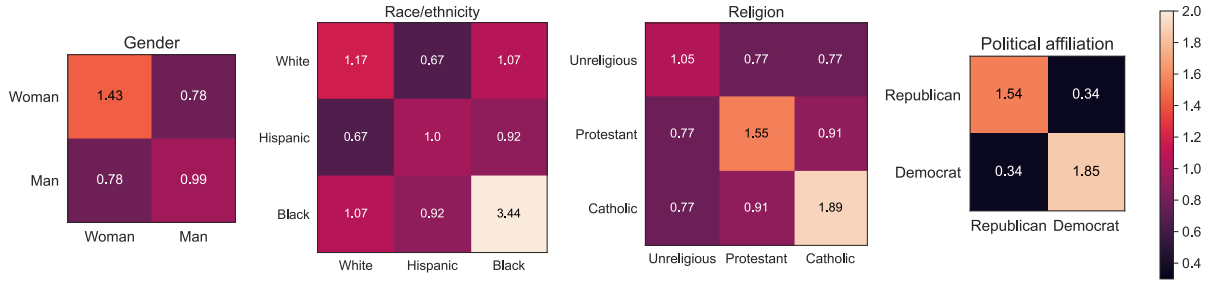


Figure 11: Ratio of observed-to-expected proportion of edges, for all pairs of demographic groups (Eq. 2). All subfigures share the same colormap (right). Groups with at least 3 nodes are kept.

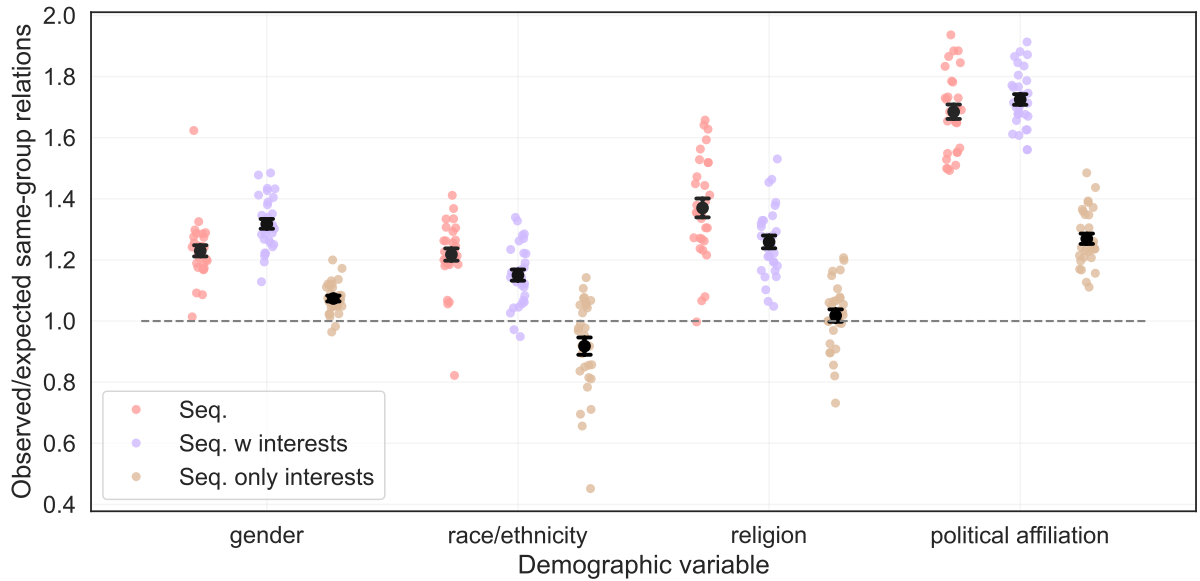


Figure 12: Visualizing demographic homophily under three methods: “Sequential” (only demographic information), “Sequential, w interests” (demographic information and interests), and “Sequential, only interests” (only interests). The LLM places the largest emphasis on political homophily in all cases.

Incorporating interests. In Figure 12, we visualize demographic homophily under three versions of the Sequential method: when only demographic information is provided, when demographic information and interests are provided, and when only interests are provided. In all cases, the LLM places the largest emphasis on political homophily.

In Table 5, we report the top interests per demographic group. The LLM generates interests as a comma-separated list (see examples in Table 2), which makes it straightforward to separate the list into individual interests and compute, for each group and interest, what percentage of personas in that group have that interest. For this experiment, we use 1,000 personas, instead to our usual set of 50 personas, so that we can estimate percentages over larger populations. We report percentages for all groups with at least 30 personas (see the counts per group in Table 7). We find that

“social justice” is a common interest across groups since it dominates Democrats’ interests (62.5%) and Democrats account for a large portion of every other group besides Republicans. We can also see the result of correlations between demographic identities: for example, men, White, and religious populations are likelier to be Republicans, resulting in higher percentages for “conservative politics”.

Real-world homophily for other demographics.

In the main text, we showed that levels of political homophily predicted by the LLM are unrealistically high, compared to reported levels of homophily in real-world social networks (Table 1). What about levels of homophily for the other demographic variables? Across the six models we test, the LLM consistently predicts homophily to be the strongest for political affiliation, followed by religion, then gender and race/ethnicity (Appendix A). Several works

Demographic group	Top interests
Man	social justice (29.1%), church activities (23.8%), conservative politics (23.4%), sports (17.1%), community service (16.7%), technology (15.7%), golf (14.0%), history (13.6%), video games (12.6%), progressive policies (11.2%)
Woman	social justice (35.3%), gardening (31.5%), community service (27.7%), reading (21.6%), church activities (20.8%), conservative politics (16.2%), volunteering (12.8%), family gatherings (11.6%), travel (10.8%), cooking (9.2%)
White	gardening (27.4%), conservative politics (25.8%), church activities (24.0%), social justice (23.0%), community service (15.9%), reading (15.6%), outdoor activities (12.0%), history (11.0%), volunteering (11.0%), golf (10.7%)
Hispanic	social justice (46.0%), community service (35.8%), family gatherings (27.3%), church activities (18.2%), cultural heritage (16.0%), music (13.4%), progressive policies (12.3%), conservative politics (12.3%), family (10.7%), soccer (10.7%)
Black	social justice (58.6%), community service (33.1%), church activities (21.1%), gospel music (17.3%), progressive policies (15.8%), community activism (14.3%), music (14.3%), reading (13.5%), jazz music (11.3%), sports (11.3%)
Asian	social justice (27.9%), travel (24.6%), technology (23.0%), church activities (16.4%), community service (14.8%), conservative politics (14.8%), yoga (13.1%), fitness (11.5%), entrepreneurship (11.5%), gardening (11.5%)
Protestant	church activities (36.1%), social justice (33.2%), community service (25.2%), gardening (22.0%), conservative politics (21.4%), reading (13.9%), sports (10.9%), volunteering (9.5%), history (9.3%), outdoor activities (8.9%)
Catholic	community service (37.7%), social justice (35.2%), family gatherings (25.5%), church activities (24.3%), conservative politics (21.5%), gardening (16.2%), reading (10.1%), sports (9.3%), volunteering (8.9%), progressive policies (8.5%)
Unreligious	social justice (28.3%), technology (22.8%), gardening (21.0%), travel (18.8%), fitness (16.3%), conservative politics (15.9%), reading (13.0%), outdoor activities (13.0%), progressive policies (12.7%), entrepreneurship (9.4%)
Republican	conservative politics (41.6%), church activities (32.1%), gardening (23.2%), outdoor activities (15.0%), golf (14.3%), community service (13.9%), sports (13.5%), family gatherings (12.7%), history (12.2%), hunting (11.4%)
Democrat	social justice (62.5%), community service (29.3%), progressive policies (18.6%), gardening (16.4%), reading (15.6%), church activities (13.2%), volunteering (12.4%), music (11.0%), travel (10.4%), technology (10.0%)

Table 5: Top 10 interests per demographic group.

agree that gender homophily should be smaller, compared to other demographic variables. For example, [McPherson et al. \(2001\)](#) says, “By the time that they are adults, people have friendship and confidant networks that are relatively sex-integrated (at least when compared to other dimensions like race, age, and education),” and [Thelwall \(2009\)](#) says, “For U.S. friendship in the last century, the key factors, in decreasing order, seem to be race and ethnicity, age, religion, educational level, occupation, and gender.”

However, these quotes also reveal that homophily for race/ethnicity should not be as low as it is for gender. For example, data from [Thelwall \(2009\)](#), who studies connections on MySpace, suggests same-group ratios of 1.96 for race/ethnicity, 1.69 for religion, and 0.96 for gender. [Smith et al. \(2014\)](#), using data from the US General Social Survey (GSS), finds ratios of 1.63 for religion, 1.32 for race/ethnicity, and 1.19 for gender in 1985 and ratios of 2.08 for religion, 1.47 for race/ethnicity, and 1.12 for gender in 2004. These numbers reveal how much variation there is in levels of ho-

mophily across studies and over time, making it difficult to evaluate whether the LLM’s levels of homophily are realistic or not. However, two trends that are clear are that gender homophily is relatively low, which the LLM does capture (although it seems to slightly overestimate), and that religion and race/ethnicity homophily should both be higher than gender homophily, the first of which the LLM captures and the second of which the LLM misses. Furthermore, the LLM’s levels of race/ethnicity homophily are 1.23 for Local and 1.22 for Sequential (using GPT-3.5 Turbo), which are below the three real-world numbers we found (1.96, 1.32, and 1.47), suggesting that the LLM may be underestimating race/ethnicity homophily, in addition to overestimating political homophily.

Model costs and comprehension. In this work, we focus primarily on realism and bias to evaluate the generated networks. However, when using LLMs, measures such as token costs and model comprehension are also very important. We measure token cost as the number of input tokens and

Method	$O(\text{input})$	# input tokens	# output tokens	Expected # turns	Actual # turns
Global, demos	$O(ND)$	607	95.267	1	1.133
Local, demos	$O(N^2D)$	30450	196.767	50	50
Sequential (friend list), demos	$O(N^2(D + E))$	42601.233	335.633	50	50
Sequential (degree), demos	$O(N^2(D + N))$	37735	200.300	50	50.033
Sequential (degree), interests	$O(N^2(I + N))$	37035	257.967	50	50.033
Sequential (degree), demos + interests	$O(N^2(D + I + N))$	57385	190.733	50	50.067

Table 6: Comparing model costs and comprehension over different LLM methods for social network generation. For Sequential, we consider two versions: listing each persona’s current friend list vs. only their current degree. N is the number of nodes in the network, E is the number of edges, and D and I are the number of tokens needed to describe all demographics and interests, respectively.

output tokens, summed over generating the entire network. We also conduct a big-O analysis of how the input tokens scale with network size, based on N (the number of nodes in the network), E (the number of edges), D (the number of tokens to describe all demographics), and I (the number of tokens to describe all interests). To measure model comprehension, we consider the expected number of turns (prompt and response) to generate the entire network, compared to the actual number of turns. The actual exceeds the expected if we could not parse the model’s response (e.g., it gave an ID that does not exist in the network). So that we can measure the concepts of cost and model comprehension independently, we only add to the number of input/output tokens on *successful* turns.

We report results in Table 6, with all measures averaged over the 30 networks generated per method. The Global method requires, by far, the fewest number of input tokens, since we only need to list all personas once. However, Global has the highest rate of errors, resulting in an actual number of turns that is 13% higher than the expected number of turns. The Local method and Sequential method scale similarly, since they both require iterating through all N personas, and for each persona, presenting them with information about the other $N-1$ personas. Their main difference is what information is provided about each persona: Sequential provides network information, which can be each person’s friend list (resulting in an additional E per iteration) or only each person’s degree (resulting in an additional N per iteration). Both Local and Sequential have good model comprehension, with

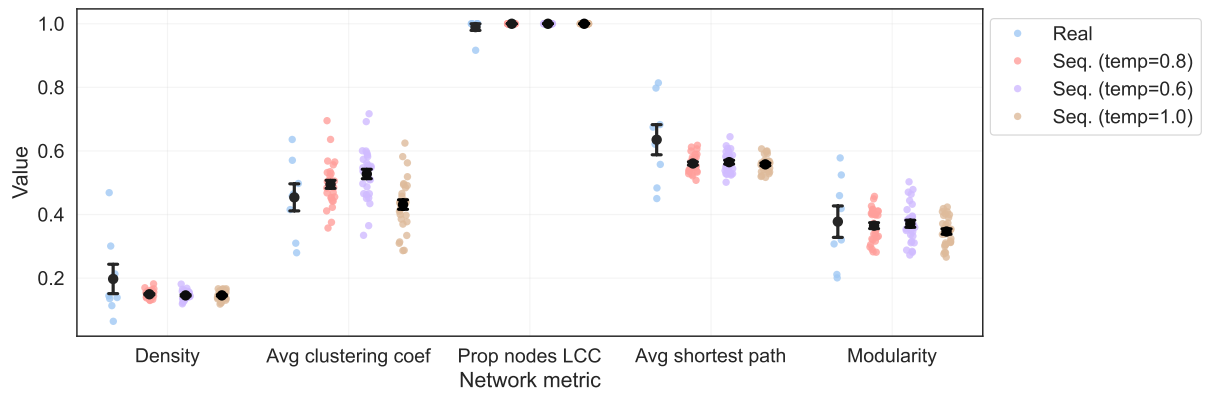
the models rarely failing and actual turns being only 0-6.7% above expected turns. Overall, this table lays out tradeoffs, since the Global method requires far fewer tokens, but as we saw in the main text (Figures 2-4), it produces much less realistic networks, and it is more prone to invalid responses.

Sensitivity analyses. In our experiments, we use a default temperature of 0.8. In Figure 13, we show that our main results do not significantly change if we use a temperature of 0.6 or 1.0 instead. Since the LLM overemphasizes political homophily, we also try adding “Pay attention to all demographics” to the system prompt. We include GPT-4o in this study as well due to its extreme levels of political homophily (Figure 7). In Figure 14, we show that adding this prompt does not significantly change results for GPT-3.5 Turbo or GPT-4o. Finally, as mentioned before, we also find that results do not significantly change if we prompt the LLM to generate a short reason for each friend that it selects. Thus, our results are robust to these perturbations in temperature and prompt.

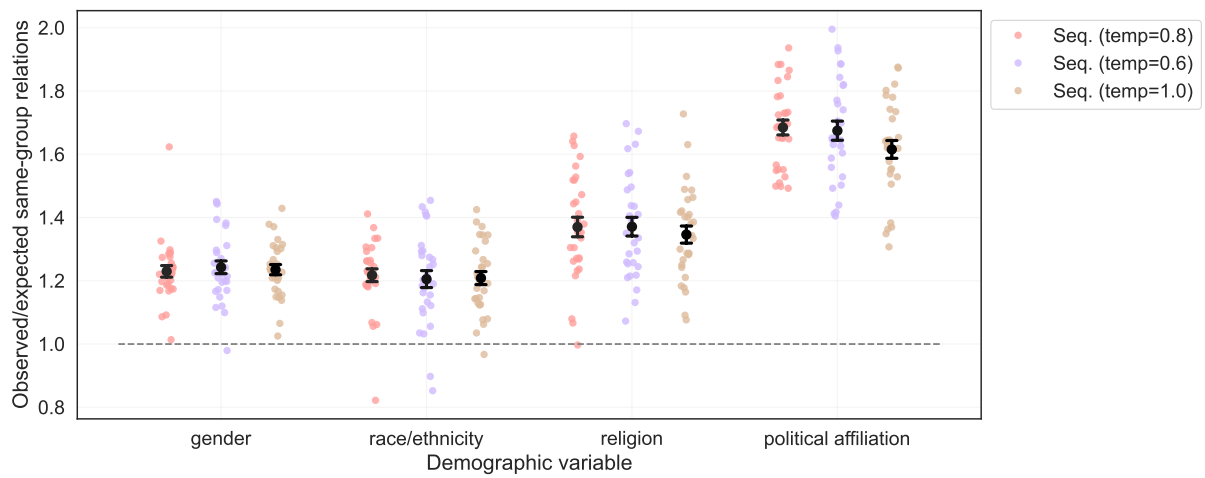
C Methodological details

C.1 Persona construction

As described in the main text, we include gender, age, race/ethnicity, religion, and political affiliation. In Table 7, we list the number of personas in each demographic group for the sample of 50 personas we used in most of our experiments, as well as the sample of 1,000 personas we used for evaluating top interests per demographic (Table 5). In Figure 15, we visualize the distribution of ages in the

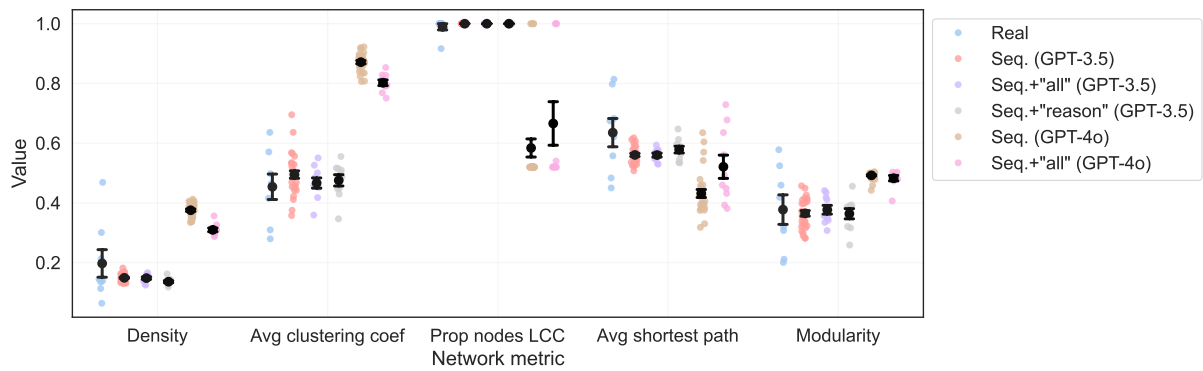


(a) Comparing structural network metrics.

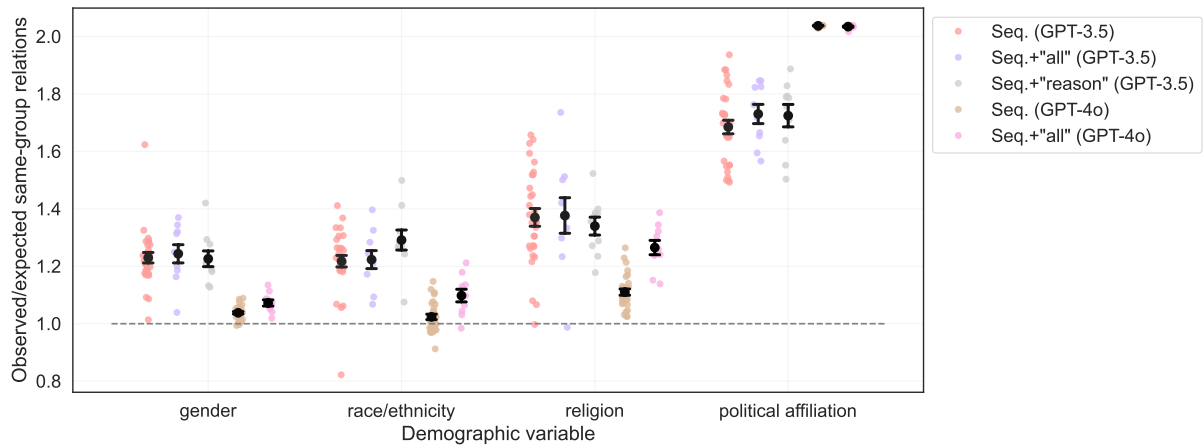


(b) Comparing homophily.

Figure 13: In our experiments, we use a default temperature of 0.8. Our main results do not change significantly if we use a temperature of 0.6 or 1.0 instead.



(a) Comparing structural network metrics.



(b) Comparing homophily.

Figure 14: Our results do not change significantly with minor changes to the prompt. We try adding “Pay attention to all demographics” (+“all”) and prompting the LLM to give a short reason for each friend that it selects (+“reason”).

Demographic	Group	Count in 50	Count in 1,000
Gender	Woman	26	499
	Man	24	492
	Nonbinary	0	9
Race/ethnicity	White	33	609
	Hispanic	10	187
	Black	4	133
	Asian	2	61
	American Indian/Alaska Native	1	9
	Native Hawaiian/Pacific Islander	0	1
Religion	Protestant	19	440
	Unreligious	20	276
	Catholic	11	247
	Jewish	0	12
	Hindu	0	9
	Buddhist	0	8
	Muslim	0	6
	Other Christian	0	2
	Political affiliation	Democrat	24
Republican		26	474
Independent		0	25

Table 7: Marginal distributions of personas’ demographics. Count in 50 indicates the number of personas belonging to each group in the sample of 50 personas we used for most experiments. Count in 1,000 indicates their number in the sample of 1,000 personas we used for evaluating top interests per demographic group (Table 5)

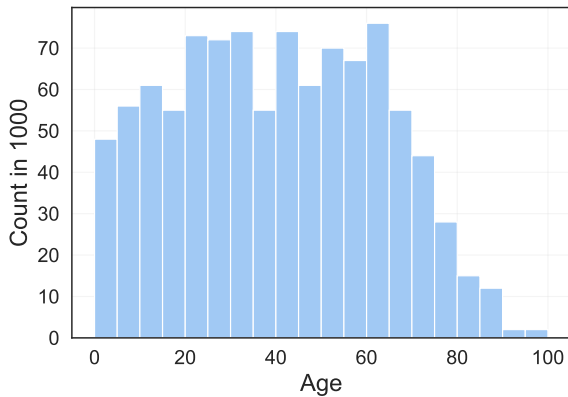


Figure 15: Age distribution in sample of 1,000 personas.

sample of 1,000 personas. Below, we explain how we sampled demographic variables per persona.

Gender, race/ethnicity, and age. First, we use data from the US Census (US Census Bureau, 2023), who provide monthly population estimates for sex, race/ethnicity, and age (individual years, from 0 to 100 years old). Specifically, we downloaded nc-est2023-alldata-r-file07.csv from US

Census datasets archived online⁸ and used the data for June 2023. We use these estimates to calculate joint distributions of gender, race/ethnicity, and age. Additionally, using data from Pew Research Center (Brown, 2022), we sample from the age-dependent distribution of those who identify as non-binary.

Religion. We sample religion conditioned on the persona’s race/ethnicity. Statista (Statista, 2016) provides distributions of religious identity for adults in the US in 2016, for most race/ethnicities. Additionally, using data from 2020 PRRI Census of American Religion (PRRI Staff, 2021), we acquire the distribution for Native Americans.

Political affiliation. Finally, we sample political affiliation conditioned on the persona’s race/ethnicity and gender. We primarily use data from Pew Research Center (Pew Research Center, 2024), using the 2023 numbers from their figure, “Partisan identification by gender among racial and ethnic groups,” which cover most race/ethnicities. Additionally, we use data from Brookings (Sanchez and Foxworth, 2022), who report Native Americans’ distribution of political support in 2022.

⁸<https://www2.census.gov/programs-surveys/popest/datasets/2020-2023/national/asrh/>

Interests. In Figure 16, we provide the prompt that we use to generate interests. We randomize the order of demographics provided, since we find that the LLM seems to pay special attention to the first listed demographic when generating interests. We use GPT-4o to generate interests, since we find that it follows the required format a little better.

C.2 Network generation

In Figures 17-19, we provide the full basic prompts for each of our network generation methods: Global, Local, and Sequential. These are the prompts that are used when only demographic variables are provided per persona. When interests are provided, we add “interests include: ...” per persona. In variants of the Sequential prompt, discussed in Appendices A and B, we experiment with specifying the number of friends that should be chosen; prompting the LLM to generate a short reason for each selected friend; and adding “Pay attention to all demographics” to the prompt.

For the Global method, the entire list of personas is given in one prompt, while in the Local and Sequential methods, the LLM is assigned one persona at the time and all other personas are listed. We generate 30 networks per method where, for each generated network, we randomize the order that the personas are listed, and, for the Local and Sequential methods, we also randomize the order in which personas are assigned (using different orders for listing and assignment). For the Sequential method, we experiment with providing each persona’s list of friends versus only their degree. We find that the model performs better with only degree, while listing friends results in unrealistically high densities. Furthermore, fewer tokens are used with only degree, so we use this version of Sequential.

C.3 Evaluating network structure

In this section, we provide more details about the real social networks that we compared against and define various measures we used to characterize the networks. In Table 8, we provide basic statistics about the real networks.

Real networks. We use the following six networks from the CASOS repository⁹:

Galesburg (Coleman et al., 1957). This network describes friendship ties between physicians, where they were asked to name three doctors whom they

⁹<http://www.casos.cs.cmu.edu/tools/datasets/external/index.php>

Network	# nodes	# edges
Galesburg	31	63
Hi-tech	36	91
Karate	34	78
Prison	67	142
Tailor 1	39	158
Tailor 2	39	223
Moreno freshmen	31	218
Moreno high school	70	274

Table 8: Summary statistics of the eight real social networks that we use.

considered personal friends and to nominate three doctors with whom they would discuss medical matters. The goal of this study was to analyze the diffusion of a new drug in terms of when physicians first prescribed it, studied in the context of their social network.

Hi-tech (Krackhardt, 1999). This network describes friendship ties between employees of a small hi-tech firm. In a survey, they answered the question, “Who do you consider to be a personal friend?” Most friendship nominations were reciprocated, and an edge is kept only if both people nominated each other.

Karate (Zachary, 1977). This network describes friendships between members of a karate club at a US university. Due to a schism where the club split into two, this network has often been used to study community structure.

Prison (MacRae Jr., 1960). This network describes friendship ties between prison inmates. All were asked, “What fellows on the tier are you closest friends with?” Each respondent could choose as many or as few friends as he desired.

Tailor (Kapferer, 1972). This network describes relations between workers at a tailor shop in Zambia (then Northern Rhodesia). The dataset includes both “instrumental” ties (work-related), which we leave out, and “sociational” ties (friendship, socioemotional), which we include. Networks were recorded twice, seven months apart, so we have two networks from this dataset.

We also include two networks from KONECT¹⁰:

Moreno freshmen. This network describes friendship ratings between university freshmen. The edge weights range from -1 (risk of getting into conflict) to +3 (best friend). We keep all edges with strictly positive weight.

¹⁰<http://konect.uni-koblenz.de/networks/>

User: In 8-12 words, describe the interests of someone with the following demographics:
race/ethnicity: White
age: 72
gender: Man
political affiliation: Republican
religion: Catholic
Answer by providing ONLY their interests. Do not include filler like "She enjoys" or "He has a keen interest in".

Figure 16: Prompt to generate interests for persona.

System: Your task is to create a realistic social network. You will be provided a list of people in the network, where each person is described as "ID. Gender, Age, Race/ethnicity, Religion, Political affiliation". Provide a list of friendship pairs in the format ID, ID with each pair separated by a newline. Do not include any other text in your response. Do not include any people who are not listed below.

User: 28. Man, age 48, Hispanic, Protestant, Democrat
11. Man, age 31, White, Protestant, Democrat
10. Man, age 58, Hispanic, Catholic, Democrat
41. Woman, age 41, White, Catholic, Republican
...

Figure 17: Prompt for Global method.

System: You are a Man, age 48, Hispanic, Protestant, Democrat. You are joining a social network. You will be provided a list of people in the network, where each person is described as "ID. Gender, Age, Race/ethnicity, Religion, Political affiliation". Which of these people will you become friends with? Provide a list of *YOUR* friends in the format ID, ID, ID, etc. Do not include any other text in your response. Do not include any people who are not listed below.

User: 11. Man, age 31, White, Protestant, Democrat
10. Man, age 58, Hispanic, Catholic, Democrat
41. Woman, age 41, White, Catholic, Republican
2. Woman, age 20, White, Catholic, Republican
...

Figure 18: Prompt for Local method.

System: You are a Man, age 48, Hispanic, Protestant, Democrat. You are joining a social network. You will be provided a list of people in the network, where each person is described as "ID. Gender, Age, Race/ethnicity, Religion, Political affiliation", followed by their current number of friends. Which of these people will you become friends with? Provide a list of *YOUR* friends in the format ID, ID, ID, etc. Do not include any other text in your response. Do not include any people who are not listed below.

User: 11. Man, age 31, White, Protestant, Democrat; has 4 friends
 10. Man, age 58, Hispanic, Catholic, Democrat; has 2 friends
 41. Woman, age 41, White, Catholic, Republican; has 0 friends
 2. Woman, age 20, White, Catholic, Republican; has 7 friends
 ...

Figure 19: Prompt for Sequential method, when only degree is provided. We also have a version where each persona’s current list of friends (in the form of ID) is provided.

Moreno high school. This network describes friendship ratings between high school boys. The edge weights range from -1 (risk of getting into conflict) to +3 (best friend). We keep all edges with strictly positive weight.

Network metrics. Most of the network metrics that we compare against are straightforward, such as density or average clustering coefficient, which are defined in the main text (Section 4). The one more involved metric is modularity, which assesses the quality of a community partition. Modularity measures the number of edges within the community, compared to how many edges are expected, and it is defined as

$$Q = \frac{1}{2E} \sum_{ij} (A_{ij} - \gamma \frac{N_i N_j}{2E}) \mathbb{1}[c_i = c_j], \quad (3)$$

where γ is the resolution parameter (set by default to 1) and c_i indicates node i ’s community in the partition. As in the main text, E is the total number of edges in the network; A_{ij} , as the adjacency matrix, is 1 if nodes i and j are connected and 0 otherwise; and N_i is i ’s number of neighbors.

We also need to define how we quantified the distance between the generated networks and real networks in Table 3. Let x_1, \dots, x_m represent the values of a metric (e.g., density) from the real networks (where $m = 8$), and let y_1, \dots, y_n represent the values of the metric from the generated networks (where $n = 30$). First, we compute the difference in their mean, divided by the standard deviation of the real network distribution:

$$D = \frac{|\frac{1}{m} \sum_{i=1}^m x_i - \frac{1}{n} \sum_{j=1}^n y_j|}{\sigma_{\text{real}}}. \quad (4)$$

We normalize by standard deviation to make differences comparable across metrics. We only normalize by the real networks’ standard deviation since normalizing by the generated networks’ standard deviation would arbitrarily reward higher variance methods. Second, we use the two-sample Kolmogorov–Smirnov (KS) statistic, which measures the distance between two empirical distributions by comparing their cumulative distribution functions (Hodges Jr., 1958):

$$\begin{aligned} F_{\text{real}}(u) &= \frac{1}{m} \sum_{i=1}^m \mathbb{1}[x_i \leq u] \\ F_{\text{gen}}(u) &= \frac{1}{n} \sum_{j=1}^n \mathbb{1}[y_j \leq u] \\ D_{KS} &= \sup_u |F_{\text{real}}(u) - F_{\text{gen}}(u)|. \end{aligned} \quad (5)$$

Comparing to classical models. We compare to several classical models for social network generation, which we describe below, along with how we chose their parameters. For all models, we set the number of nodes, N , to 50, to mimic our LLM experiments with 50 personas. We use the networkx implementation for all three models.¹¹

Erdős–Rényi random graph (Erdős and Rényi, 1959). We use the $G_{N,p}$ random graph model, which has N nodes and each edge is included with independent probability p . In our experiments, we simply set p to the average density of the eight real social networks.

Barabási–Albert preferential attachment (Barabási and Albert, 1999). In this model, one

¹¹<https://networkx.org/documentation/stable/reference/generators.html>

node is added to the graph at each step, and it forms m edges with existing nodes, where each neighbor is sampled with probability proportional to its current degree. The networkx implementation starts by default with a star graph on $m + 1$ nodes, then adds the remaining $N - m - 1$ nodes one at a time. Thus, the number of edges in the graph is always $m + ((N - m - 1) \cdot m)$. We choose $m = 5$, which minimizes the difference between the generated graph’s density and the average density of the real social networks.

Watts-Strogatz small world (Watts and Strogatz, 1998). In this model, first a ring is created over N nodes, then each node is joined to its k nearest neighbors, forming a lattice. Then, with independent probability p , each edge (i, j) is rewired, meaning it is replaced with (i, j') , where j' is selected from all nodes (aside from i and i ’s existing neighbors) uniformly at random. Since each node is joined to its k nearest neighbors, the number of edges in this graph is always $\frac{nk}{2}$. So, we choose $k = 10$, which also minimizes the difference between the generated and real networks’ average density. Then, with $N = 50$ and $k = 10$, we sweep over possible values of p in $\{0.01, 0.02, \dots, 0.5\}$ to minimize the difference between the generated and real networks’ average clustering coefficient, resulting in $p = 0.15$.

C.4 Evaluating homophily

To compare the LLM’s level of political homophily to prior work, we needed to use their measures of homophily. First, we define the isolation index, used in Halberstam and Knight (2016) and Gentzkow and Shapiro (2011). We define it following Halberstam and Knight (2016) (Appendix, p. 5). First, for voter $j \in J$ (they refer to all nodes in their network as voters), let v_{jC} and v_{jL} indicate their number of conservative and liberal followers, respectively. Then, isolation is defined as

$$\begin{aligned} \text{share-C}_j &= \frac{v_{jC}}{v_{jC} + v_{jL}} \\ \text{C-exposure}_i &= \frac{1}{\sum_{j \in J} A_{ij}} \sum_{j \in J} A_{ij} \cdot \text{share-C}_j \\ \text{C-exposure}_t &= \frac{1}{N_t} \sum_{i \in I_t} \text{C-exposure}_i \\ \text{isolation} &= \text{C-exposure}_C - \text{C-exposure}_L \end{aligned} \quad (6)$$

Thus, C-exposure_i for a voter i is the average share-C_j over the voters that they follow, C-exposure_t

is the average conservative exposure for voters in group t , and isolation is the difference in average conservative exposure for conservative versus liberal voters.

We also use the polarization measure from Garimella and Weber (2017). First, they compute the user’s leaning, l , which is

$$l = \frac{\alpha}{\alpha + \beta},$$

where α and β indicate how many left-leaning and right-leaning users, respectively, are followed by this user. Specifically, they begin with a uniform prior, $\alpha = \beta = 1$, then every follow/retweet of a user on each side adds one to that side’s parameter (α for left, β for right). Note that their definition of leaning is very similar to the definition of share-C_j in Halberstam and Knight (2016), with the addition of the uniform prior. Then, their definition of polarization p is

$$p = 2 \cdot |0.5 - l|, \quad (7)$$

which lies between 0 and 1, representing how much the user deviates from a balanced leaning of 0.5. They report average p over users, which is what we measure on our networks as well.